TECHNICAL UNIVERSITY OF LIBEREC
Faculty of Mechatronics, Informatics
and Interdisciplinary Studies

Preparation of nanomaterials from a complex of gold salt and cyclodextrin

Bachelor thesis

Study programme: N0719A270001 – Nanotechnology
Study branch: N0719A270001NA – Nanotechnology

Author: **Ondřej Novák**
Supervisor: M.Sc. Rafael Omar Torres Mendieta, Ph.D.
Consultant: Ing. Sabrin Issam Abdallah

Liberec 2024

TECHNICKÁ UNIVERZITA V LIBERCI
Fakulta mechatroniky, informatiky
a mezioborových studií

Preparation of nanomaterials from a complex of gold salt and cyclodextrin

Bakalářská práce

Studijní program: N0719A270001 – Nanotechnologie
Studijní obor: N0719A270001NA – Nanotechnologie

Autor práce: **Ondřej Novák**
Vedoucí práce: M.Sc. Rafael Omar Torres Mendieta, Ph.D.
Konzultant: Ing. Sabrin Issam Abdallah

Liberec 2024

FAKULTA MECHATRONIKY,
INFORMATIKY A MEZIOBOROVÝCH
STUDIÍ TUL

Bakalářská práce

Preparation of nanomaterials from a complex of gold salt and cyclodextrin

Studijní program: B0719A130001 Nanotechnologie
Autor práce: **Ondřej Novák**
Vedoucí práce: Dr. Rafael Torres
Ústav nových technologií a aplikované informatiky

Konzultant práce: Ing. Sabrin Issam Abdallah
Oddělení environmentální chemie

Liberec 2024

FAKULTA MECHATRONIKY,
INFORMATIKY A MEZIOBOROVÝCH
STUDIÍ TUL

Zadání bakalářské práce

Preparation of nanomaterials from a complex of gold salt and cyclodextrin

Jméno a příjmení:	**Ondřej Novák**
Osobní číslo:	M21000080
Studijní program:	B0719A130001 Nanotechnologie
Zadávající katedra:	Katedra chemie
Akademický rok:	2023/2024

Zásady pro vypracování:

An objective of this bachelor's thesis is to utilize conventional wet chemical techniques for the creation of a gold-cyclodextrin complex.
Within the implementation of the current research work, we also aim to investigate the usage of the synthesized gold-cyclodextrin complex as a starting material for its transformation into gold nanomaterials through the laser-based methodology known as laser synthesis of colloids. This goal primarily involves delving into the necessary synthetic conditions and parameters to achieve the formation of these nanomaterials.
Lastly, we will perform an extensive characterization of the newly created nanomaterials. To achieve this, we will utilize various analytical techniques, including scanning electron microscopy (SEM), dynamic light scattering (DLS), and ultraviolet-visible (UV-Vis) spectroscopy, among others.

Rozsah grafických prací:	dle potřeby dokumentace
Rozsah pracovní zprávy:	50 stran
Forma zpracování práce:	tištěná/elektronická
Jazyk práce:	angličtina

Seznam odborné literatury:

1. LIU, Zhichang, et al. Selective isolation of gold facilitated by second-sphere coordination with α-cyclodextrin. Nature Communications, 2013, vol. 4, no 1, p. 1855.
2. LIU, Zhichang, et al. Cation-dependent gold recovery with α-cyclodextrin facilitated by second-sphere coordination. J. Am. Chem. Soc., 2016, vol. 138, no 36, p. 11643-11653.
3. LIU, Wenqi, et al. Supramolecular gold stripping from activated carbon using α-cyclodextrin. J. Am. Chem. Soc., 2020, vol. 143, no 4, p. 1984-1992.
4. JURCEK, Ondrej, et al. Heads or tails? Sandwich-type metallo complexes of Hexakis (2, 3-di-O-methyl)-α-cyclodextrin. Crystal Growth & Design, 2020, vol. 20, no 6, p. 4193-4199.
5. PROCHOWICZ, Daniel, et al. Interactions of native cyclodextrins with metal ions and inorganic nanoparticles... Chemical reviews, 2017, vol. 117, no 22, p. 13461-13501.
6. PONCHEL, Anne; MONFLIER, Eric. Application of cyclodextrins as second-sphere coordination ligands for gold recovery. nature communications, 2023, vol. 14, no 1, p. 1283.
7. ZHANG, Dongshi; GOKCE, Bilal; BARCIKOWSKI, Stephan. Laser synthesis and processing of colloids: fundamentals and applications. Chemical reviews, 2017, vol. 117, no 5, p. 3990-4103.
8. TORRES-MENDIETA, Rafael, et al. Laser-assisted synthesis of Fe-Cu oxide nanocrystals. Applied Surface Science, 2019, vol. 469, p. 1007-1015.
9. ETTEL, David, et al. Laser-synthesized Ag/TiO nanoparticles to integrate catalytic pollutant degradation and antifouling enhancement... Applied Surface Science, 2021, vol. 564, p. 150471.
10. FRIAS BATISTA, Laysa M., et al. Generation of nanomaterials by reactive laser-synthesis in liquid. Science China Physics, Mechanics & Astronomy, 2022, vol. 65, no 7, p. 274202.
11. HAVELKA, Ondřej, et al. Reactive laser ablation in acetone towards phase-controlled nonequilibrium Iron-and Nickel-Bi2O3 nanoalloys. Applied Surface Science, 2023, p. 158503.

Vedoucí práce:	Dr. Rafael Torres Ústav nových technologií a aplikované informatiky
Konzultant práce:	Ing. Sabrin Issam Abdallah Oddělení environmentální chemie
Datum zadání práce:	11. října 2023
Předpokládaný termín odevzdání:	14. května 2024

L.S.

prof. Ing. Zdeněk Plíva, Ph.D.
děkan

prof. Ing. Josef Šedlbauer, Ph.D.
garant studijního programu

V Liberci dne 13. listopadu 2023

Prohlášení

Prohlašuji, že svou bakalářskou práci jsem vypracoval samostatně jako původní dílo s použitím uvedené literatury a na základě konzultací s vedoucím mé bakalářské práce a konzultantem.

Jsem si vědom toho, že na mou bakalářskou práci se plně vztahuje zákon č. 121/2000 Sb., o právu autorském, zejména § 60 – školní dílo.

Beru na vědomí, že Technická univerzita v Liberci nezasahuje do mých autorských práv užitím mé bakalářské práce pro vnitřní potřebu Technické univerzity v Liberci.

Užiji-li bakalářskou práci nebo poskytnu-li licenci k jejímu využití, jsem si vědom povinnosti informovat o této skutečnosti Technickou univerzitu v Liberci; v tomto případě má Technická univerzita v Liberci právo ode mne požadovat úhradu nákladů, které vynaložila na vytvoření díla, až do jejich skutečné výše.

Současně čestně prohlašuji, že text elektronické podoby práce vložený do IS/STAG se shoduje s textem tištěné podoby práce.

Beru na vědomí, že má bakalářská práce bude zveřejněna Technickou univerzitou v Liberci v souladu s § 47b zákona č. 111/1998 Sb., o vysokých školách a o změně a doplnění dalších zákonů (zákon o vysokých školách), ve znění pozdějších předpisů.

Jsem si vědom následků, které podle zákona o vysokých školách mohou vyplývat z porušení tohoto prohlášení.

13. května 2024 Ondřej Novák

Abstract

The current bachelor's thesis focuses on the chemical synthesis of needle-shaped $KAuBr_4$ complex with α-cyclodextrins, followed by their utilization as precursors in the reactive laser ablation in liquids (RLAL) technique for generating nanoparticles with non-spherical morphologies. RLAL involves the use of a pulsed laser to irradiate a solid plate, such as gold, immersed in a liquid medium, extracting nanoparticles from it. Within this process, the suspended complexes in the liquid act as growth-directing agents, guiding the formation of gold nanoparticles post-extraction through ablation. As a result, the emerging nanoparticles exhibit altered shapes compared to the typically spherical gold nanoparticles obtained without the addition of complexes. A crucial observation is that the creation of genuinely small nanoparticles, including clusters, plays a pivotal role in shaping, influenced by the presence of these complexes. These needle-shaped complexes efficiently capture such small particles, thus impacting the final nanoparticle morphology. The success of this endeavor heavily hinges on identifying optimal method parameters, particularly laser intensity. The use of a femtosecond laser at maximum power significantly degrades the precursor complexes due to their organic carbon composition. Consequently, adjustments to the gold plate's position relative to the laser were implemented to prevent direct ablation at the focal distance after focusing the laser beam. This modification effectively reduces laser intensity during experimentation, creating more conducive conditions for the cyclodextrin complexes. Furthermore, this reduction facilitates the generation of small particles and clusters during ablation, primarily occurring in the evaporation phase of the process. Through this methodology, non-spherical nanoparticles were synthesized successfully, albeit without precise control over their resulting shapes. Essentially, this research introduces a novel approach to shape-modified nanoparticle synthesis, employing cyclodextrin complexes as growth-directing precursors within an RLAL framework.

Keywords: gold nanoparticles, cyclodextrins, laser synthesis in liquids, reactive laser ablation, chemical growth control, shape-modified nanoparticles

Abstrakt

Tato bakalářská práce se zaměřuje na chemickou syntézu jehličkovitých komplexů KAuBr4 s α-cyklodextriny, následovanou jejich využitím jako prekurzorů v technice reaktivní laserové ablace v kapalinách (RLAL) pro generování nanočástic s nekulatými morfologiemi. RLAL zahrnuje použití pulzního laseru pro ozáření pevného plíšku, jako je zlato, ponořeného do kapalného média, čímž se z ní extrahují nanočástice. V rámci tohoto procesu fungují suspendované komplexy v kapalině jako řídící látky růstu, které řídí formování zlatých nanočástic po extrakci prostřednictvím ablace. V důsledku toho mají vznikající nanočástice modifikované tvary ve srovnání s typicky kulatými zlatými nanočásticemi získanými bez přidání komplexů. Klíčovým pozorováním je, že vytvoření opravdu malých nanočástic, včetně klastrů, hraje zásadní roli v tvarování, ovlivněné přítomností těchto komplexů. Tyto jehličkovité komplexy efektivně zachycují takové malé částice, čímž ovlivňují konečnou morfologii nanočástic. Úspěch tohoto úsilí značně závisí na identifikaci optimálních parametrů metody, zejména intenzity laseru. Použití femtosekundového laseru na maximální výkon významně degraduje prekurzorové komplexy kvůli jejich organické uhlíkové povaze. Kvůli tomu byla provedena úprava pozice zlatého plíšku vůči laseru, aby se zabránilo přímé ablaci v ohniskové vzdálenosti po zaostření laserového paprsku. Tato modifikace účinně snižuje intenzitu laseru během experimentování, čímž vytváří příznivější podmínky pro cyklodextrinové komplexy. Navíc toto snížení usnadňuje generování malých částic a klastrů během ablace, které se převážně odehrává ve fázi vypařování procesu. Tímto způsobem byly úspěšně syntetizovány nekulaté nanočástice, i když bez přesné kontroly nad jejich vznikajícími tvary. Souhrnně řečeno, tato práce představuje nový přístup k syntéze nanočástic modifikovaného tvaru, který využívá cyklodextrinové komplexy jako řídící prekurzory v rámci RLAL.

Klíčová slova: nanočástice zlata, cyklodextriny, laserová syntéza v kapalinách, reaktivní laserová ablace, chemické řízení růstu, nanočástice modifikovaného tvaru

Acknowledgements

I would like to express my gratitude to my thesis supervisor, Rafael Torres, PhD., for his guidance, valuable advice, continuous openness to collaboration and consultation, and patience throughout the completion of this thesis. I deeply appreciate the opportunity to work with him, learn from him, and be part of his research team. I would like to specifically thank him for his insightful introduction to the various aspects of academic research and for his assistance with the analyses.

I would also like to thank my consultant, Ing. Sabrin Abdallah, for her help and advice during the experiments and the processing of results, and the thesis itself. Her friendly approach made the preparation of this work an enjoyable experience.

Furthermore, I would like to thank Associate Professor Michal Řezanka, PhD., and his team from the Department of Nanochemistry, specifically Ing. Pavlína Konopáčová for her help in the laboratory, and Christopher Hobbs for the NMR analysis of the samples. Last but not least, I greatly value the opportunity to conduct research at the laboratories of the Institute for Nanomaterials, Advanced Technologies, and Innovation (CxI).

The authors acknowledge the assistance provided by the Research Infrastructure NanoEnviCz, supported by the Ministry of Education, Youth and Sports of the Czech Republic under Project No. LM2023066.

Also, artificial intelligence (ChatGPT by OpenAI) is acknowledged as it was utilized for ensuring English accuracy and refining the stylistic aspects of the text.

Immense thanks are also due to my family, led by my mom, who has supported me in everything as she always has, allowing me to pursue my interests and enjoyments, not just in academic work.

Contents

List of abbreviations

CD	Cyclodextrin
CLAL	Continuous Laser Ablation in Liquids
CxI	Institute for Nanomaterials, Advanced Technologies, and Innovation
demiH2O	Demineralized Water
ELAL	Electric Field-Assisted Laser Ablation in Liquids
LAL	Laser Ablation in Liquids
LPL	Laser Pyrolysis in Liquids
LSPC	Laser Synthesis and Processing of Colloids
LSL	Laser Synthesis in Liquids
MAS	Magic Angle Spinning
NMR	Nuclear Magnetic Resonance
NP	Nanoparticle
PLAL	Pulsed Laser Ablation in Liquids
RLAL	Reactive Laser Ablation in Liquids
SEM	Scanning Electron Microscopy
SLAL	Sequential Laser Ablation in Liquids
SPR	Surface Plasmon Resonance
SSNMR	Solid-State Nuclear Magnetic Resonance
UV	Ultraviolet
UV-Vis	Ultraviolet-visible

List of Figures

1 Introduction

Nanoparticles (NPs) are becoming increasingly important in a wide range of fields, including medicine, electronics, and energy production [1, 2]. Their small size enables them to exhibit unique properties and behaviors that are not seen in larger materials. However, the properties and behavior of NPs can vary greatly depending on their shape, size, and surface properties [3]. Therefore, it is essential to control these factors when producing NPs for specific applications. By controlling the shape and properties of NPs, researchers can tailor their performance to specific applications. This is particularly important in medicine, where NPs can be designed to target specific cells or tissues in the body, leading to more effective treatments with fewer side effects [4]. Developing methods for creating NPs with specific shapes and properties is, thus, crucial for unlocking the full potential of these materials in various fields.

Nowadays, there are various methods for creating NPs with specific shapes and properties. These methods include the use of conventional chemical techniques that leverage physical and chemical laws to predict the appearance and structure of the nanomaterials being produced. The basic classification of preparation methods is based on how the NPs themselves are created [5]. The first approach is the top-down method, where particles are generated from a larger bulk material that exceeds nanoscale dimensions [6]. This can involve various lithographic techniques such as cutting, etching, grinding, and ball milling, where the material is sufficiently crushed to produce NPs [7, 8, 9]. The top-down approach essentially means reducing the size of the structure to the nanoscale. Another approach is the bottom-up method, which is primarily based on the arrangement or even self-assembly of basic chemical entities on the nanoscale into larger units. Examples include a cell using enzymes to create DNA by taking building molecules and joining them together to form the final component or the phenomenon of chemical precipitation, which is the formation of a separable solid from a solution either by converting the substance into an insoluble form or by changing the solvent composition to reduce the solubility of the substance in it [10].

Reactive laser ablation in liquids (RLAL) [11, 12] is a method that lies at the boundary between the two fundamental approaches to nanoparticle preparation, the aforementioned “top-down” and “bottom-up”. The basic principle of the method involves generating smaller particles by focusing the laser beam on larger material.

However, a closer look reveals that after the particles detach from the bulk due to laser irradiation, a series of mechanisms that definitely belong to the bottom-up approach principles come into play. Initially formed atomic clusters gradually form into larger and more cohesive NPs, which fits exactly into the description of the bottom-up technique. One of the main focuses of this work is the use of a combination of both approaches, specifically the methods of chemical co-precipitation and laser ablation in liquids. The goal of this methodology is to obtain NPs of different shapes than usual. We aim to bring new insights into the science of this yet fully unexplored possibility of preparing nanomaterials of various shapes and structures and, thus, properties. We focus on using chemically prepared precursors in nano to micro dimensions as part of the liquid environment, in which NPs are subsequently formed using a laser. In our case, the liquid environment is not a pure solvent but a colloidal solution. The subject of interest is how such modification of the liquid environment during laser ablation can affect the resulting NPs, especially their shape.

The shape of NPs plays a crucial role in nanotechnologies as it affects their physical and chemical properties and significantly impacts their applications in various fields. The shape of NPs is influenced by a number of factors, including energetic factors, synthesis conditions, and the structure of the molecules of the starting material. Energetic factors, such as surface energy and interaction energy between atoms or molecules, play a key role in determining the preferred shape of NPs [13]. For example, spherical NPs are often the most stable and energetically favorable, whereas nanowire structures are suitable for electronic applications [14, 15]. Gold NPs, which are part of this work, most commonly appear spherical due to these energetic factors in nanomaterials. Such particles are often prepared chemically, just like many other elements. However, the disadvantage of this approach is the poor transferability of procedures to other materials. Different materials require the use of various chemical agents and possibly different individual laboratory operation conditions, not to mention the frequent need to use toxic chemical substances to obtain final NPs [16]. RLAL, in contrast, offers a suitable alternative for both shortcomings. At the same time, the preparation of particles avoids the use of toxic agents.

When it comes to gold in nano size, various shapes are achievable. In the study from which this bachelor's thesis is derived, gold is part of a complex forming nano-needles. Based on the work [17, 18], where the authors managed to create nano-objects with needle-like shapes using gold salt and cyclodextrins (CDs) in an aqueous environment. The authors, in their work under the auspices of Nobel laureate J. Fraser Stoddart, present a method and results of preparing these structures using gold salt complexes composed either of bromide or chloride anions and cations of potassium, lithium, cesium, or rubidium, and α-, β-, or γ-CDs. Chemical co-precipitation in the experiments was observed only in three of the 24 possible combinations, and the combination of $KAuBr_4$ and α-CD showed the highest yield. The prepared nanoobjects correspond to 1D cable superstructures formed by alter-

nately arranged $(K(OH_2)_6)^+$ and $(AuBr_4)^-$ in ionic conductors wrapped in α-CD toruses head-to-tail and tail-to-tail (see Fig. 1.1). In terms of structure, there is an arrangement where CDs act as second sphere ligands, with the potassium cation placed between their heads, and on the other side, the bromide anion is contained between the tails in the structure. The authors present the possibility of using this knowledge of the structure and properties of the resulting NPs for eco-friendly gold mining. For the current thesis work, $KAuBr_4$ and α-CD particles were prepared as initial precursors for their subsequent use in laser irradiation of a gold target in the environment of a colloidal solution of these particles.

It can be assumed that after using these nanostructures in the form of an aqueous suspension as a liquid environment in RLAL will result in the production of NPs that differ from those that would have been formed in a pure water environment. Our primary focus is on the difference in morphology and overall shape of the NPs prepared in this manner. This implies that the precursors, in the form of nano-needles in suspension, have an impact on the newly forming NPs when subjected to a laser, thereby allowing us to alter the shape of the resulting NPs.

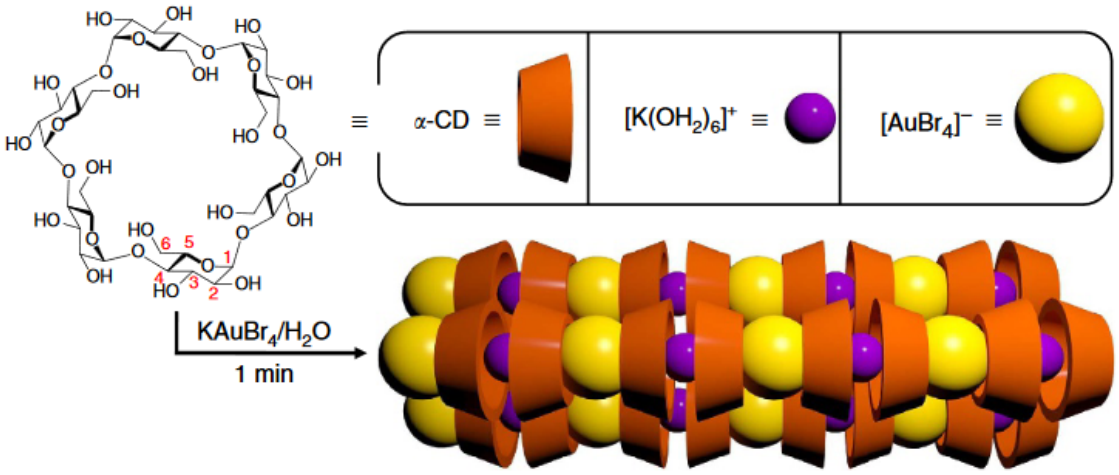

Figure 1.1: Visualization of structure of $KAuBr_4$ and α-CD complex. The cavities of the α-CDs oriented head-to-head, tail-to-tail form a continuous channel, which is filled by an alternating $(K(OH_2)_6)^+$ and $(AuBr_4)^-$ polyionic chain to generate a cable-like superstructure [19].

2 Theoretical background

2.1 Nanomaterials

When we explore objects that have at least one dimension on the scale of $10(^{-9})$ meters, we refer to them as nanomaterials. The word "nano" comes from the Greek word "nanos", which translates to "dwarf" [20]. Since a standard school ruler's smallest division is 1mm, dividing it into 1,000,000 smaller pieces would be needed to reach a scale of 1nm. Hence, studying objects of such size requires specialized methods and tools capable of handling such diminution.

The history and development of nanotechnology are a fascinating tale of human curiosity and innovation. From the first use of the term "nanotechnology" by physicist Norio Taniguchi in 1974 [20] to Richard Feynman's seminal lecture "There's Plenty of Room at the Bottom" [21], the evolution of nanotechnology has come a long way. This progress has not only pushed the boundaries of what is scientifically discoverable and technologically feasible but has also opened new avenues in medicine, electronics, materials science, and many other fields.

As we delve into the realm of nano dimensions, we must consider the physical behavior of this environment. As dimensions decrease, we enter a sphere where the physical descriptions familiar from the macroscopic environment falter, requiring greater reliance on laws and predictions provided by quantum mechanics. The principles of quantum mechanics underlie a vast array of observational and analytical methods that yield a plethora of diverse data for the characterization of nanomaterials. The contribution of quantum mechanics to the understanding and utilization of nanomaterials cannot be overstated. Fundamental quantum phenomena such as quantum tunneling effect or quantum dot structures are crucial for the properties and behavior of materials on the nanoscale. These phenomena enable the development of new semiconductor devices, quantum computers, and highly sensitive sensors that utilize the unique properties of nanomaterials. In Professor Dr. Emil Roduner's manuscript entitled "Size Matters: Why Nanomaterials Are Different" [22], he states from the outset that, regarding nanomaterials, there are basically two types of size-dependent effects: smoothly scalable ones related to the fraction of atoms at the surface and quantum effects that show discontinuous behavior due to the completion of shells in systems with delocalized electrons.

In addition to quantum phenomena, surface phenomena are also significant in nanomaterials, often relating to properties and interactions between objects themselves and with the environment. In the context of nanomaterials, the advantage of a large specific surface area is often discussed, defined as the ratio of surface area to volume [23].

The quantum nature mainly pertains to a closer description of NPs or clusters. Nanomaterials are not synonymous with NPs; they are just one of the possible forms. How nanomaterials are classified and how they differ is explained in subsequent chapters. Among the most basic types of materials include NPs, as well as nanolayers, nanoalloys, and also objects whose dimensions exceed the nanoscale but are made up of parts (cells) that correspond to nano dimensions [5, 24].

The versatility of nanomaterials is evident in their applications across various fields. In medicine, they enable targeted drug delivery, enhance diagnostic methods, and minimize side effects [4]. In electronics, they facilitate device miniaturization, improve performance, and enhance energy efficiency [1, 15]. In materials engineering, they contribute to the development of stronger, lighter, and more durable materials, with applications in aviation, automotive, and construction industries [25]. These examples underscore the transformative potential of nanomaterials in traditional industries [20].

2.1.1 Basic classifications

Nanomaterials are a diverse group of materials that can be classified based on various aspects and properties. This chapter introduces some of the fundamental categorizations that are useful across different focuses and applications of nanomaterials. The chapter also briefly discusses the classification of NPs based on shape. It is important to note that the term “nanomaterials” is sometimes specifically referred to as “NPs” in this chapter. This is because many synthesis methods deal with and describe the synthesis of NPs, and therefore, most sources present procedures for preparing such objects. NPs are often considered as building blocks for other distinct types of nanomaterials, such as nanolayers, nanocomposites, or polycrystals.

One way to classify nanomaterials is based on their origin. Natural materials like protein molecules or milk, as an example of a colloid, occur spontaneously in the natural realm. In contrast, artificial nanomaterials are created by humans using targeted procedures and methods.

Dimension-based classification is another common way to categorize nanomaterials. The dimension of an object is perhaps the most fundamental property suitable for independent description, whether in the macro world or at the nano level. Nanomaterials are divided according to their dimension as follows (see Fig. 2.1) [5]:

- 0D materials: All three dimensions of the examined object are at the nanoscale, with values typically in the range of nanometers. Examples include NPs, quantum dots, or fullerenes.
- 1D materials: Only two of the three dimensions are at the nanoscale, with the third dimension significantly exceeding and described in micrometers. However, it could be even larger than micrometers, crucial for this classification is that the dimension surely exceeds approximately 100 nm. Examples are mostly needle-like structures such as nanorods, nanotubes, nanowires, or nanofibers.
- 2D materials: Here, only one of the dimensions remains at the nanoscale, suggesting that these objects are likely planar. These include nanolayers, thin coatings, or nanowalls. However, examples from 1D materials that retain a needle-like shape but have dimensions exceeding the nanoscale boundary also fall into this category.
- 3D materials: These materials include objects that exceed nanometric values in all dimensions, but their building blocks are precisely 0D, 1D, and 2D nanomaterials. This could be a bulk material composed of nanocubes and would fit into this classification. Examples include multi-nanolayers, bundles of nanotubes/nanowires, or core-shell structures.

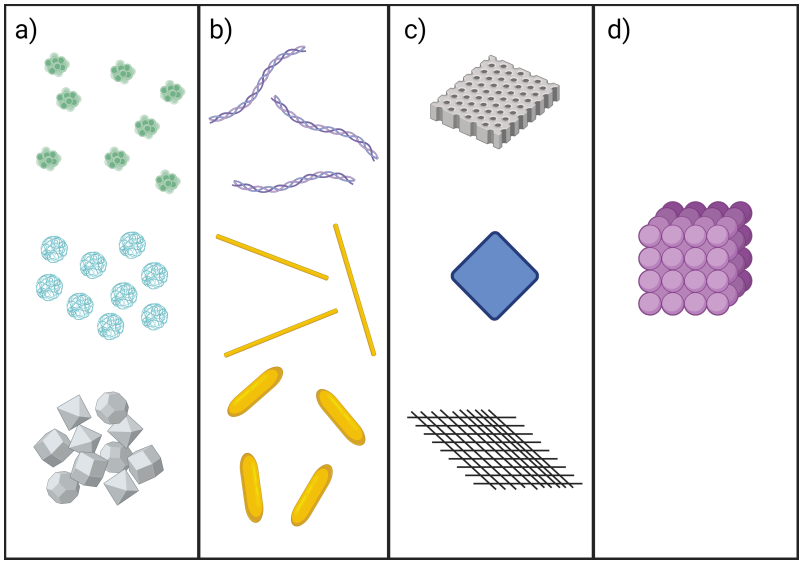

Figure 2.1: Dimension-based classification, a) 0D clusters, spheres and nanodiamonds, b) 1D nanofibers, nanowires and nanorods, c) 2D membrane, film and network and d) 3D nanocrystal cube.

Another possible way to classify nanomaterials is by composition. Organic nanomaterials, including representatives like liposomes, dendrimers, and micelles, are one

category [26]. Inorganic nanomaterials can be further divided into metal-based [27], metal oxides [28], semiconductors [29], and ceramics. Carbon-based nanomaterials are another extensive category, made up of carbon structures like fullerenes [30], carbon nanotubes [31], graphene [32], carbon nanofibers [33], and carbon black [34]. Lastly, composite nanomaterials are made up of NPs of different kinds, from NPs with larger particles to nanomaterials combined with some bulk material [35].

Properties of materials are also a criterion for the classification of nanomaterials, for example, by chemical, physical, optical, or mechanical properties. Finally, nanomaterials differ in the way they are prepared.

When it comes to the shape of NPs, there are countless possibilities. From common spherical shapes to intricate morphological structures like nanoflowers, the variety of shapes and structures of NPs is vast. Spherical NPs are the most stable and energetically favorable due to their minimized surface energy, making them ideal for medical applications as they can easily traverse biological barriers [36]. However, NPs can assume diverse shapes and the underlying factors for this are energetic considerations, synthesis conditions, and internal structure, all of which have significant implications for their practical applications in various fields.

Cylindrical NPs, such as nanotubes, have a unique shape dictated by the internal structure and arrangement of atoms or molecules. These structures are often harnessed for their conductive properties in electronics, exemplifying the profound influence of internal structure on nanoparticle shape [37]. NPs with a branched structure exhibit higher surface energy due to a larger number of surface atoms or molecules, a characteristic that significantly influences their behavior and potential applications [38]. Dendritic NPs, similar to dendrites in nature, have a branched structure that can be useful for medical applications [39]. Meanwhile, polyhedral NPs, typical for metallic NPs, can take various geometric forms, such as cubes, cuboctahedra, or double tetrahedra [40]. Lastly, nanowires are elongated structures that can vary in length and diameter and are frequently used in electronics for their conductive properties [15].

A detailed look at typical inorganic NPs includes spherical, pseudo-spherical, dodecahedral, tetrahedral, octahedral, cubic, and corresponding hollow morphologies for 0D structures; nanotubes, nanoneedles, nano-screws, nanocapsules, and hollow structures for 1D morphologies; and discs, hexagonal/triangular/square plates, ribbons, hollow spheres, hollow rings, and others for 2D morphologies. Complex shapes like nano-urchins, nanoflowers, nanostars, and others are included in 3D morphologies [41].

The variety of shapes and structures of NPs opens doors for designing materials with precisely defined properties [42]. For example, while spherical NPs may be ideal for medicinal purposes due to their ability to easily penetrate biological

barriers, tubular or fibrous NPs find their use in reinforcing composite materials or as components of nano-electronic devices. The surface of NPs can either be uniform [43] or differ through various modifications [44]. In terms of structure, NPs can be crystalline [45] or amorphous, each influencing their application differently [46].

2.1.2 Nanoparticles

Nanoparticles (NPs) belong to a category of nanomaterials known as 0-D materials, which typically have dimensions in the tens of nanometers or less in each direction. Due to their small size, NPs exhibit unique and remarkable properties that are often a result of their size. For instance, the melting point, conductivity, and optical characteristics of NPs are all influenced by their particle size. One visible consequence of particle size affecting these properties is the color of the colloidal solution containing the NPs. This phenomenon is fundamentally a result of the small dimensions of the particles and their interaction with light. The visible spectrum of electromagnetic radiation spans wavelengths approximately from 380 nm to 740 nm. Particles whose sizes are similar to the wavelength values of specific electromagnetic radiation will naturally interact differently with light than objects that are significantly larger or smaller. So, in the study of nanomaterials, the color a material displays at the macroscopic scale or in bulk form may not correspond to the color observed when NPs are made from this material. Although a single particle is imperceptible to the naked eye, in a colloidal solution containing a large number of NPs, the color becomes a useful indicator of certain information. At a minimum, it serves as a quick and often initial indicator that NPs are present in the solution.

Apart from particle size, the shape of NPs also plays a crucial role in nanotechnologies as it affects their physical and chemical properties and significantly influences their applications in various fields. To fully harness these unique nanostructure properties, synthetic methods must be developed for the rational control of their size, shape, and composition. Although shape has proven to be one of the most useful parameters for tailoring the properties of NPs, it has also been one of the most challenging to control intentionally [47].

There are many reasons for the diverse shapes of NPs, but the most crucial include energetic factors and synthesis conditions where variables like temperature, pressure, concentration, and type of solvent affect the nanoparticle formation process and the molecular structure of the starting material itself. Nature shows us that virtually all systems operate to achieve a state of lowest possible energy while being energetically stable. Since energy is the universal currency of the universe, every system seeks to reach an energy state where it is "satisfied". The shape of NPs is the result of efforts to minimize surface energy while maximizing the energy stability of the entire structure [13]. Occasionally, concepts like mass and surface energy are introduced to better describe these phenomena, which are key parameters influencing the shape of NPs.

Efforts to predict and control particle shape often arise from thermodynamic aspects and kinetics. The concept of a nanoparticle's thermodynamic equilibrium shape is directly related to determining the minimum total energy. Wulff constructions are used as a method to find the shape of NPs with minimal energy. A Wulff shape is defined as a set of points that meet certain conditions regarding surface free energy and crystallographic orientation [13]. Insights gained from these models can help predict shapes and particles, thus enhancing the understanding of their properties' origins, which in turn can lead to information on potential applicability. While equilibrium shapes of NPs are obtained using various Wulff constructions, kinetic shapes arise from kinetic growth. Kinetic models are helpful for both qualitative and, fundamentally, quantitative predictions of nanoparticle shapes. They are determined by growth rates, with different shapes potentially differing from equilibrium shapes [13]. The initial step of growth is always nucleation, which may be homogeneous or heterogeneous, depending on conditions and the environment. This is followed by growth, which can occur in various ways. There is a dynamic between the formation of new structures during growth and a return to thermodynamically stable shapes. At the end of growth, NPs may fall into one of three classes: dominated by thermodynamic equilibrium, kinetics, or stochastic [13]. Since one of the most common shapes, NPs adopt is spherical, the "shape factor" can be used to describe them [48], which is defined as the ratio of the surface area of a non-spherical nanoparticle to the surface area of a corresponding spherical nanoparticle, both with the same volume.

The synergistic effects of thermodynamic and kinetic aspects are crucial in determining the final shape of inorganic NPs. However, predicting and controlling their shape remains challenging due to the unpredictable changes caused by even slight variations in reaction conditions. As a result, the shape control of inorganic NPs largely remains empirical. While there are no simple rules for determining the final shape of these nanomaterials, advancements in computational technology and microscopy are leading to the development of predictive theories [41].

Another important aspect of NPs is their large specific surface area (see Fig. 2.2). Due to their small size, the ratio of surface area to volume in NPs is significantly greater than that of bulk materials. For example, a diced cube with a 1 cm edge has a surface area of 6 cm^2, while dividing it into smaller cubes with 1 nm edges would result in a surface area of 6000 m^2, a seven-order-of-magnitude increase. This property enables NPs to interact more efficiently with their surrounding environment, allowing for greater molecule adsorption on the surface of NPs. This is particularly important in applications such as catalysis and sensing [49], where the large specific surface area enhances the efficiency of catalytic reactions and enables the detection of low concentrations of analytes due to the high reactivity of the nanoparticle surface.

The potential applications of NPs are vast and varied, ranging from the healthcare and food industry to textiles and electronics. For instance, NPs of zinc oxide or

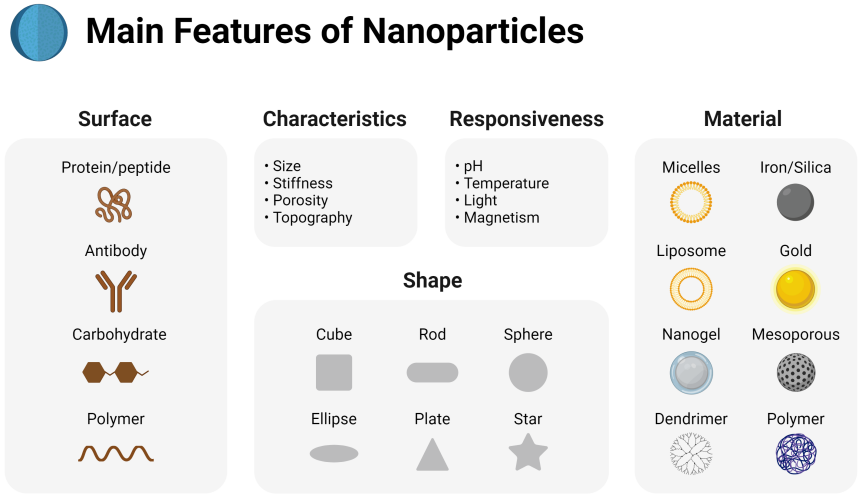

Figure 2.2: This infographic categorizes the primary characteristics of nanoparticles into five main groups: Surface modifications, intrinsic physical characteristics, responsiveness to environmental stimuli, material composition, and geometric shapes.

titanium dioxide are used in cosmetics and sunscreens to provide effective UV protection without leaving white marks on the skin. In electronics, NPs are utilized to develop high-performance, flexible, and transparent electronic circuits, paving the way for the creation of flexible displays and solar panels. Other applications include catalysis, medicine, and the food industry. These innovative, versatile materials hold immense potential for the future [28, 50, 3].

Gold NPs

Gold NPs possess distinct properties that set them apart from bulk gold, thanks to the manifestation of quantum effects at small particle sizes. These effects, particularly pronounced at the nanometer level, lead to gold NPs exhibiting significantly different absorption and scattering characteristics compared to bulk gold. The size and shape of the NPs directly influence the energy levels of surface electrons, resulting in changes in light absorption and scattering. This unique behavior allows for a wide range of practical applications, such as enhancing the performance of optical sensors and improving therapeutic methods, thereby demonstrating the real-world relevance of gold NPs at the nanoscale [51, 52, 53].

The phenomenon driving all these properties is known as plasmonic resonance, which occurs when light interacts with free electrons on the surface of NPs [54]. Specifically, plasmonic resonance happens when free electrons on the surface of NPs resonate in response to light waves. The shape of NPs plays a crucial role in the localization and intensity of Surface Plasmon Resonance (SPR), allowing specific tuning of optical properties. The influence of shape on SPR can be explained using

electromagnetic field theory. Depending on the shape of the NPs, there is a different localization and distribution of surface charges, which directly impacts the resonant frequency. For example, spherical NPs exhibit simple resonant bands, while rod-shaped or star-shaped NPs have more complex spectral characteristics with multiple resonant modes (see Fig. 2.3). Changing the shape of NPs from spheres to ellipsoids or rods can lead to a shift in the resonant peak to shorter wavelengths. This effect is caused by an increased surface distribution of electrons, which is more effective in interacting with light. There is also an increased electromagnetic field localization at NPs with sharp edges, which can lead to a stronger and more narrowly focused SPR [55, 56]. Specific tuning of SPR by modifying the shape of gold NPs allows for creating more effective sensors and better-targeted medical applications. In biosensing, precise resonance tuning can detect specific biomolecules with high sensitivity and selectivity [57]. In photovoltaics, specific resonance tuning can increase the efficiency of converting light energy into electrical current [58].

The historical context of using gold in colloidal solutions by Michael Faraday [59] and subsequent theoretical developments underscore gold's longstanding interest and significance at the nanoscale. Current methods for preparing gold NPs include top-down and bottom-up approaches, with laser ablation in liquids being a promising method for generating NPs of specific shapes and sizes. Various reaction conditions and additives in the laser ablation process can influence the morphology and composition of the resulting NPs, allowing for the creation of NPs with targeted properties for specific uses [60]. In the current thesis, we are exploiting such a fact by modifying the liquid environment where NPs will be created by molecules able to direct nucleation processes, like CDs, which have recently been found to exert these processes by harnessing second-sphere coordination [17, 18].

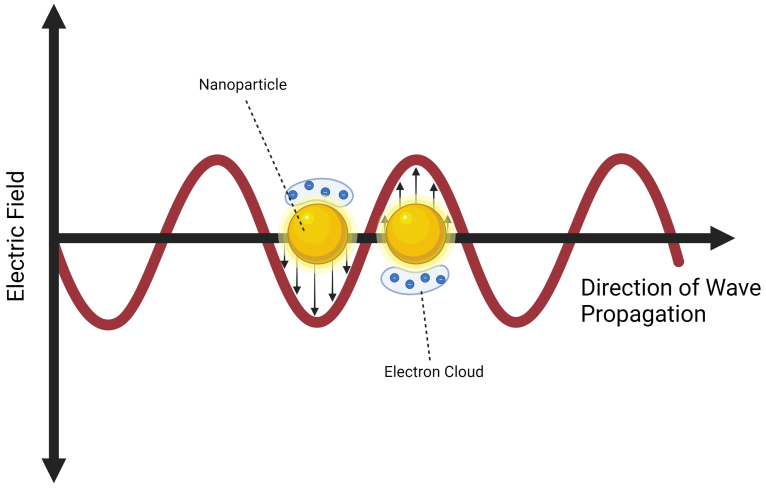

Figure 2.3: Scheme of SPR on the surface of NPs visualizing changes of intensity of electric field, which happens in the direction of wave propagation

2.2 Preparation methods

Although various methodologies can be employed for synthesizing gold NPs with non-spherical shapes, e.g. co-precipitation, our focus is a combination of two very new and versatile methods for growing these types of nanostructures, RLAL and Template-Assisted Synthesis with CDs. Recent studies have found that CDs can direct the growth of nanoparticles by harnessing second-sphere coordination. By controlling the concentration and orientation of CDs in solution, it is possible to tailor the shape of gold NPs synthesized via chemical reduction methods. This approach offers a versatile and environmentally friendly route to producing gold NPs with well-defined non-spherical shapes, such as nanorods, nanoprisms, and nanoflowers [61]. Additionally, the use of laser ablation in liquids, involving using a laser to ablate a gold target submerged in a liquid medium, typically water or an organic solvent, can be employed to vaporize the gold target, generating a plasma plume containing gold atoms and ions. The rapid cooling and condensation of this plasma result in the formation of gold NPs, which, if surrounded by growth director molecules as CDs, could result in NPs with diverse shapes, including nanorods, nanostars, nanocubes, and other non-spherical morphologies (see Fig. 2.4) [62]. On top of this, RLAL provides a clean and efficient method for producing nanomaterials without the need for toxic reducing agents.

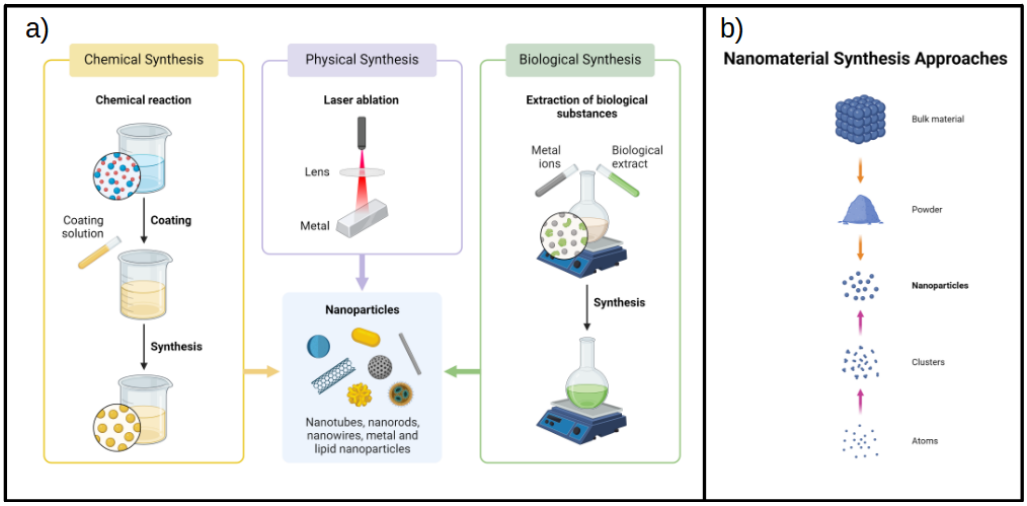

Figure 2.4: Visualizations of NM synthesis approaches. a) This diagram illustrates the three principal approaches to nanoparticle synthesis: chemical, physical, and biological. Chemical synthesis involves chemical reactions such as coatings to produce nanoparticles. Physical synthesis, shown here using laser ablation, relies on physical forces to generate nanoparticles from metals. Biological synthesis utilizes biological extracts and metal ions to create environmentally friendly nanoparticles [63]. b) Synthesis of NMs is often divided into “top-down” and ”bottom-up” approaches. Their basic hierarchical breakdown is illustrated in this diagram showing a few major checkpoints of synthesis.

2.2.1 Laser synthesis

When it comes to synthesizing nanomaterials by lasers, the liquid environment offers a safer and more straightforward context than air. This setting can be classified within both the "top-down" and "bottom-up" synthesis approaches to nanomaterial preparation, depending on the specific stage of the process and the ongoing phenomena under consideration. This method is commonly referred to by the acronym LSPC, denoting "laser synthesis and processing of colloids."

Laser synthesis in liquids, a key component of LSPC, harnesses laser radiation to trigger reactions within a liquid medium, forming colloidal NPs. This method distinguishes itself by its capacity to produce NPs without requiring high temperatures or toxic chemicals, thereby providing an environmentally friendly alternative to conventional synthesis techniques. LSPC involves directing a laser onto a liquid solution containing metal salts or other chemical precursors. The absorption of laser radiation induces a localized temperature rise, facilitating the reduction of metal ions and the nucleation of NPs. Consequently, NPs rapidly grow in colloidal form. A pivotal feature of LSPC lies in its ability to meticulously regulate the size, shape, and composition of NPs through precise adjustment of laser parameters and properties of the liquid medium [11].

Within the realm of LSPC, specialized methodologies exist. Laser ablation in liquids (LAL) entails employing a laser to vaporize a target material (typically solid) into a liquid environment, culminating in NP formation. This process enables direct NP synthesis without the requirement for additional chemical-reducing agents, ensuring high purity of the resulting product [64]. Photoreduction employs a laser to induce chemical reductions in solutions containing metal salts, forming reduced metal NPs. This versatile technique can synthesize metal NPs, including silver, gold, and platinum [65, 66, 67]. Laser pyrolysis in liquids (LPL) focuses on the chemical decomposition of organic precursors within a liquid environment at elevated temperatures generated by the laser, thereby facilitating the production of carbon nanostructures such as quantum dots and carbon nanotubes [68].

An overarching advantage of LSPC is its ability to produce NPs at room temperature and atmospheric pressure. This presents a notable safety and environmental benefit compared to methods like chemical synthesis, which may necessitate high temperatures, pressure, or toxic substances. Moreover, this approach obviates the requirement for surface ligands that could obstruct and contaminate NP surfaces, aligning with the principles of green chemistry [11].

LSPC is distinguished by its remarkable technological adaptability, allowing for seamless transitions between different NP types. This versatility, coupled with the potential for process automation, enhances both safety and production efficiency [69, 12, 60].

2.2.2 Laser ablation in liquids

LAL stands out as a prominent subset of LSPC methods, prized for its simplicity and adaptability in NP production. This technique employs a laser to target a solid precursor material, typically a thin metal plate or foil submerged in a liquid medium. Upon interaction with a laser (typically pulsed laser sources with pulses in the temporal region of ns, ps, or fs), the target material undergoes ablation, ejecting atoms, ions, and clusters into the liquid environment, where they coalesce to form NPs [60].

At its core, LAL operates through the absorption of intense laser radiation, typically in the form of pulses, by the target material, inducing rapid heating, melting, and eventual vaporization. The resulting ejected material undergoes cooling and condensation in the surrounding liquid, giving rise to NPs formation. The LAL process unfolds in three distinct stages: the plasma phase, the cavitation bubble phase, and the dispersion phase, where NPs interact or react with liquid molecules. Laser-material interaction within the liquid disrupts surface chemical bonds, leading to electron ejection via multiphoton ionization and the formation of hot plasma. Plasma formation necessitates surpassing the ablation threshold, indicative of the minimum energy density required. Subsequently, the collapse of the hot plasma emits substantial energy into the surrounding liquid, generating a thin vapor layer that rapidly expands to form a cavitation bubble. The bubble's transient existence, lasting on the order of hundreds of microseconds, may create a liquid microjet dispersing the formed NPs. This cyclic process recurs with each successive laser pulse [11].

The properties of NPs, including size, shape, and composition, can be finely adjusted by manipulating various parameters, such as laser wavelength, pulse duration, and energy, in addition to the choice of liquid medium. The latter is particularly influential in determining the final NP size and distribution curve during nucleation and growth phases, where diverse solvents significantly impact energy dissipation and cooling rates of ablated materials [70]. Laser type and parameters, including wavelength, power, and pulse duration, also play a crucial role in the LAL process. Pulsed lasers (PLAL) typically outperform continuous lasers (CLAL) to avoid undesirable heating of ablated material and liquid boiling. Laser wavelength determines ablated particle size and LAL process efficiency, with shorter wavelengths producing smaller particles at the expense of reduced laser power efficiency. Pulse duration is another key parameter, with shorter pulses optimizing heat exchange and precision in NP synthesis [71].

LAL is not a static technique, but one that is constantly evolving and being refined through specialized variations. Sequential Laser Ablation in Liquids (SLAL) is one such variation, enabling layer-by-layer material ablation for precise NP synthesis and layering [72]. Electric Field-Assisted Laser Ablation in Liquids (ELAL) is another, which uses an electric field to guide ablated particle movement and deposition,

thereby enhancing control over NP distribution [73]. Reactive Laser Ablation in Liquids (RLAL) is a variation that initiates post-ablation chemical reactions within the liquid medium to modify NPs' chemical composition or surface properties [74]. These variations demonstrate the adaptability and versatility of the LAL technique.

RLAL

In RLAL, the focus is on leveraging the reactive environment within the liquid medium to synthesize NPs. This innovative approach amalgamates the physical phenomenon of laser ablation with concurrent chemical reactions occurring within the liquid medium, presenting a distinctive avenue to customize both the chemical composition and surface functionalities of the resultant NPs.

RLAL involves ablating a target material with a laser beam in a liquid medium infused with reactive species or inherently reactive. The high-energy environment engendered by laser radiation not only triggers the ablation of the target material but also instigates chemical reactions between the ablated material and the reactive species dispersed in the liquid. This synergistic process can yield NPs bearing specific chemical compositions, coatings, or functional groups unattainable via conventional LAL methodologies. The tunability of NP properties via RLAL hinges upon the adjustment of diverse parameters, including the type of target material, the composition of the reactive liquid medium, and laser parameters such as wavelength, pulse duration, and energy. The selection of reactive species within the liquid medium assumes particular significance, dictating the nature of ensuing chemical reactions and thereby influencing the composition and surface functionality of the resultant NPs [70].

One of the key advantages of RLAL over traditional LAL methodologies is its ability to directly fabricate functionalized NPs during the synthesis process. By carefully selecting reactive liquid media, NPs can be synthesized with tailored surface chemistries, making them immediately suitable for specific applications without the need for subsequent modification steps. This streamlined synthesis and functionalization process not only simplifies NP production but also reduces costs, enhancing the efficiency of generating NPs for a wide range of applications [12].

2.2.3 Use of Cyclodextrins as NPs growth directors

The structural organization of CDs allows them to form inclusion complexes with a broad spectrum of guest molecules, substantially modifying the guest entities' physical, chemical, and biological attributes. In the realm of nanotechnology, especially in the crafting and creation of nanomaterials, CDs have emerged as crucial ligands. Their distinct toroidal shape and capability to encapsulate guest molecules render them a precious asset in nanotechnology for stabilizing substances and managing the release of pharmaceuticals. The formation and inclusion of complexes critically depend on non-covalent interactions between the CDs and guest molecules,

such as hydrophobic interactions, hydrogen bonds, and Van der Waals forces [75]. This offers a gentle method to adjust the behavior of NPs without compromising their structural integrity.

While the role of non-covalent interactions in creating complex units has been noted, generally, the bonding between CDs and nanomaterials can occur through various mechanisms. Covalent bonds involve the chemical attachment of CDs onto the surface of NPs through reactive groups. Non-covalent interactions, including hydrogen bonds, Van der Waals forces, and hydrophobic interactions, are fundamental and allow the physical adsorption of CDs onto the nanoparticle surface without the need for chemical modification. Furthermore, supramolecular bonds leverage the capability of CDs to form host-guest complexes with functionalized areas on the nanoparticle surface [76].

In the realm of second-sphere coordination, CDs as ligands offer a versatile and unique approach to the design and synthesis of coordination complexes. This type of interaction, where CDs do not directly coordinate with the metal center but instead influence its properties through supramolecular interactions with ligands already bound to the metal, can have a profound impact on the stability, reactivity, and selectivity of coordination complexes. The use of CDs in second-sphere coordination is not limited to a specific set of organic ligands, but rather, it extends to a wide range of ligands, thereby modulating their spatial arrangement and electronic properties [77]. This versatility in the use of CDs in second-sphere coordination opens up new possibilities in the design of functionalized materials and nanostructures, and on top of this, studies illustrate how CDs can be utilized to create complex structures with metals and contribute to the development of more sustainable and environmentally friendly methodologies for growing NPs with controlled shapes [19, 75]. Therefore, if employed during RLAL as functionalization agents, CDs could potentially act as NP growth directors, allowing the formation of NPs with non-spherical shapes.

3 Characterization techniques

To gather information about the synthesized nanomaterial, various techniques were employed, including UV-Vis spectroscopy, scanning electron microscopy (SEM), and nuclear magnetic resonance (NMR). UV-Vis spectroscopy facilitated the study of absorbance and stability in the colloidal solutions prepared using laser methodology. The SEM technique enabled the observation of the shape and morphology of the created NPs. NMR was primarily utilized for characterizing the structure of the precursor complexes.

3.1 UV-Vis Spectroscopy

UV-Vis spectroscopy, or ultraviolet-visible spectroscopy, stands as a pivotal analytical technique utilized in characterizing nanomaterials. This method relies on the absorption of light within the ultraviolet and visible regions of the electromagnetic spectrum to unveil the optical properties of materials at the nanoscale. It essentially operates on the fundamental principle of light interaction with electrons within a molecule; UV-Vis spectroscopy entails the absorption of light at specific wavelengths. When photons encounter electrons, they can prompt transitions to higher energy levels, resulting in characteristic absorption peaks in the spectrum. The resultant absorption spectrum serves as a window into the electronic structure and chemical bonds present within the material [78].

In the realm of nanomaterials, UV-Vis spectroscopy provides invaluable insights into parameters like size, shape, and composition. Variations in the size and shape of NPs notably impact their optical characteristics, as evidenced by shifts in absorption spectra. For instance, altering the size of gold NPs can induce shifts in the absorption maximum towards longer wavelengths [56]. UV-Vis spectroscopy, in addition, boasts several advantages, including its rapidity, minimal sample preparation requirements, and potential for quantitative analysis. These attributes render it adept at swiftly and effectively analyzing a broad spectrum of nanomaterials. Nonetheless, the technique may fall short in offering intricate details regarding the structural complexity of materials, thereby prompting the need for complementary characterization methods such as electron microscopy or Raman spectroscopy.

3.1.1 Absorbance

UV-Vis spectroscopy-based assessment of nanomaterials absorption spectra facilitates accurately determining absorption maxima and intensity across wavelengths. This yields crucial insights into the electronic structure and chemical bonds in nanomaterials. Given the profound influence of size, shape, and chemical composition on the optical properties of NPs, comprehending these characteristics is paramount for advancing research, serving as a means to track such alterations, and furnishing indispensable data for further analysis and application exploration [79]. In addition to qualitative analysis, UV-Vis spectroscopy enables quantitative assessment. Beer's law (Equation 3.1), for instance, facilitates the estimation of NP concentration in a sample based on measured absorption, making it a valuable tool for quality control and quantification in industrial applications requiring precise material specification.

$$A = \epsilon c d \tag{3.1}$$

, where A is absorbance (a.u.), ϵ is coefficient of absorption ($M^{-1}cm^{-1}$), d is the optical distance between irradiation source to cuvette with solution (cm) and c is a concentration of the solution (M).

In the case of metallic NPs, SPR is assessed using UV-Visible spectroscopy, which involves observing the absorbance and scattering spectra of plasmonic NPs. This technique entails passing light across the UV to visible spectrum through a sample containing NPs. The wavelengths at which these particles absorb and scatter light are then recorded as spectral data. The SPR phenomenon, characterized by a distinct peak in the absorbance spectrum, occurs due to the collective oscillation of electrons on the surface of the metal NPs when they interact with light at specific wavelengths. When NPs are non-spherical, such as rods or ellipsoids, the symmetry of the particle alters the distribution of surface electrons, thereby affecting the plasmon resonance conditions. Non-spherical particles exhibit multiple plasmon modes; for instance, nanorods have transverse and longitudinal plasmon resonances. The longitudinal mode, where the oscillation of electrons aligns with the longer dimension of the rod, typically appears at longer wavelengths compared to the transverse mode. The aspect ratio (length to diameter) of non-spherical particles significantly influences the SPR peak. Higher aspect ratios lead to a redshift (a move toward longer wavelengths) in the SPR peak, especially in the longitudinal mode, due to increased electron path length. Moreover, the non-spherical shape generally results in a broader SPR peak due to the inhomogeneous distribution of the electromagnetic field around the particle, causing variations in the local dielectric environment [55, 56].

3.1.2 Stability

Another crucial application of UV-Vis spectroscopy is in monitoring the stability of NPs over time. This technique is instrumental in tracking changes in the absorption spectrum of samples, providing vital insights into their stability and reactivity. For instance, when studying colloidal solutions of NPs, any deviation in the absorption maximum signals potential agglomeration or degradation of the particles. This underscores the importance of UV-Vis spectroscopy in our research.

This absorption peak is sensitive to several factors, including the size, shape, and state of aggregation of the NPs. Their size heavily influences the position of the absorption maximum in the spectrum of NPs. This is particularly true for NPs made of materials like gold or silver, which exhibit localized SPR. The resonance frequency, and hence the absorption maximum, shifts depending on the size of the NPs. If the NPs agglomerate (cluster together), the effective size of these clusters will be larger than that of the individual NPs, potentially shifting the absorption maximum to longer wavelengths.

The shape and structure of NPs also affect their optical properties. Any change in shape due to agglomeration or degradation can lead to changes in the absorption spectrum, for example, as a shift in the absorption spectrum [80]. Agglomeration leads to a reduction in the surface area to volume ratio of the NPs. It also affects the electromagnetic interactions between particles. These changes can result in broadening and shifting of the absorption peak. Broadening occurs because the agglomerated particles might not be uniform, leading to a spread of size and shape, which in turn causes a range of resonance conditions [81]. Degradation of NPs can alter the material's electronic structure and surface chemistry. This alteration can affect how the NPs interact with light, thereby causing a shift in the absorption maximum [82].

Therefore, UV-Vis spectroscopy emerges as an indispensable tool for assessing the long-term stability of nanomaterials, a critical aspect for their successful application across diverse fields. With its versatility, UV-Vis spectroscopy facilitates the examination of how various factors impact the stability of NPs, including temperature, pH, ionic strength, and the presence of different biological molecules [83]. This broad range of factors that can be analyzed in absorption spectra aids in identifying optimal storage and application conditions for NPs, sparking curiosity about the potential applications of this technique.

3.2 SEM

SEM stands as a cornerstone technique for delving into nanomaterials' intricate surface and structure. This method empowers researchers to capture high-resolution

images with depth contrast, pivotal for scrutinizing NP morphology, dimensions, and dispersion.

SEM, at its core, operates by scanning a sample with a beam of high-energy electrons. This process triggers diverse interactions, including backscattered electrons, secondary electrons, and characteristic X-ray radiation. These interactions are then detected and translated into images, providing insights into the topography, composition, and other physical attributes of the sample. SEM's real power lies in its ability to visualize nanostructures with meticulous detail at the nanometer scale. For instance, in the study of NPs, SEM offers precise details regarding their geometry, size, and surface characteristics, which are crucial for a wide range of applications, from drug delivery systems to solar cells [84].

SEM boasts several advantages, foremost among them its capability to generate high-resolution images with depth contrast, facilitating a comprehensive understanding of sample surface topography. Moreover, SEM enables relatively swift analyses with the potential for sample manipulation during scanning. However, it's worth noting that SEM necessitates sample conductivity, often requiring special preparation such as coating with a thin metal layer. Additionally, SEM may not be suitable for samples prone to instability in a vacuum or susceptible to damage from the electron beam (see Fig. 3.1) [85].

Undoubtedly, SEM emerges as an indispensable asset in the realm of nanotechnology, providing vital insights for advancing nanomaterials. Its knack for visualizing structures at the nanoscale fosters a more profound comprehension of material properties, laying the groundwork for innovations across a spectrum of technological domains.

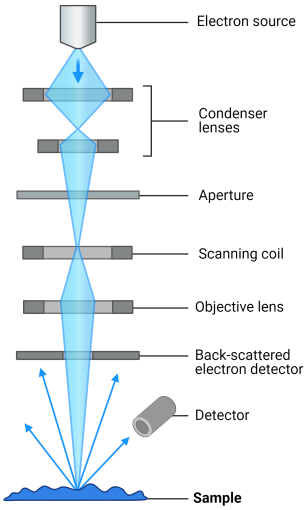

Figure 3.1: Basic scheme of SEM setup.

3.3 NMR

NMR is an indispensable analytical technique for unraveling molecular structures and dynamics, and it has extended its reach to the realm of nanomaterials. In nanotechnology, NMR serves as a powerful tool, offering unparalleled insights into the structural, dynamic, and chemical attributes of atoms within nanomaterials. Notably, it excels in scrutinizing polymeric and biological nanosystems.

NMR capitalizes on the behavior of atomic nuclei in response to an external magnetic field. Under the influence of a strong magnetic field, nuclei with non-zero spin align themselves along the field direction. Upon exposure to radiofrequency radiation at a specific frequency, select nuclei transition to a higher energy state. Subsequently, upon cessation of the radio signal, these nuclei relax back to their ground state, emitting detectable energy for analysis. The quality and utility of NMR data hinge on various factors, including the magnetic field's uniformity, the magnet's strength (quantified in Tesla), and the detector's sensitivity. A higher magnetic field yields superior resolution and sensitivity, which is critical for dissecting complex nanomaterials prone to signal overlap [86].

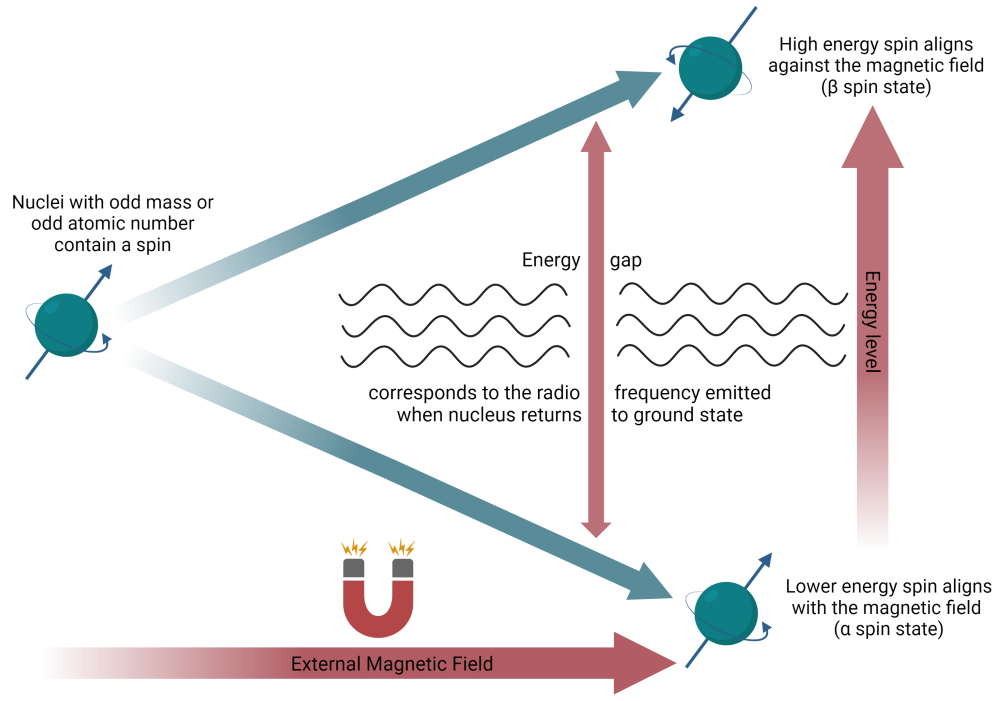

Figure 3.2: Illustration of principles used in NMR.

Within the domain of NMR, Solid-state NMR (SSNMR) emerges as a specialized branch dedicated to scrutinizing solid materials. Unlike its solution counterpart, SSNMR furnishes intricate insights into the structure, dynamics, and chemical composition of materials in their solid-state facet, which is crucial for unraveling the

mysteries of nanomaterials. SSNMR employs a repertoire of specialized techniques to augment resolution and spectrum interpretation. Foremost among these is magic angle spinning (MAS), a method that narrows resonance line widths by rapidly rotating the sample at 54.7 degrees relative to the magnetic field direction. This technique is invaluable in mitigating dipolar interactions between nuclei, yielding sharper and more intelligible spectra (see Fig. 3.2) [87].

In the realm of nanotechnology, NMR serves as a linchpin for characterizing material structures and porosities. Techniques such as SSNMR open vistas for exploring disordered systems, including amorphous polymers and, facilitate the characterization of nanostructured catalysts and the analysis of interphase interactions in nanocomposites, making it an ideal analytical method for assessing modifications in CD structure, which, as hypothesized in the current thesis, could lead to the formation of non-spherical NPs when employed as NPs growth directors in RLAL.

4 Methodology

4.1 Materials

The following chemicals and materials were used during the experiments.

- Potassium tetrabromoaurate(III) hydrate; 398454-1G; PCode: 1003435964; Source MKCQ8570; CAS-No: 13005-38-4; SIGMA-ALDRICH, Co., Spruce Street, St. Loius, MO 63103 USA
- α-Cyclodextrin; C36H60O30; CAS 10016-20-3 >98,0 %; C0776; Lot.: 57LEDDO; Mfr.: TOKYO CHEMICAL INDUSTRY CO., LTD. 6-15-9 TOSHIMA, KITA-KU, TOKYO, JAPAN
- Gold foil; >99,99 % Au, 0,5 mm, SIGMA-ALDRICH, USA
- Triple distilled water (18.2 MΩcm)

4.2 Preparation of precursors

In the preparation of the precursors, consisting of $KAuBr_4$ and an α-cyclodextrin (α-CD) complex, we adhered to the methodology outlined in Ref. [17] This article details the synthesis of these CD-based complexes for gold recovery purposes. Notably, the authors meticulously explored various experimental conditions, including temperature adjustments, to optimize yield and solubility. The practical synthesis of the precursors involved precise steps. Initially, 11.1 mg of $KAuBr_4$ and 38.9 mg of α-CD were weighed. These substances were then combined in a 4 ml vial containing 2 ml of distilled H_2O. Sequentially, $KAuBr_4$ was introduced into the vial, followed by the addition of H_2O, and subsequently α-CD. A magnetic stir bar facilitated stirring as the reaction progressed for 20 minutes under standard laboratory conditions.

The emergence of a faint cloudiness within the first minute indicated the formation of the CD complex in the orange colloidal solution (Figure 5.1). Given the foundational nature of this synthesis, it was repeated iteratively. Occasionally, adjustments were made to the quantities of reactants employed. To upscale production, all components were doubled, employing 22.2 mg of $KAuBr_4$, 77.8 mg of α-CD, and 4 ml of H_2O.

4.3 Laser irradiation

Following the preparation of the colloidal solution of $KAuBr_4$ with α-CD as a precursor for RLAL, experimental procedures involving laser irradiation commenced. A gold foil immersed in the aqueous medium of the precursor solution was situated within a laser chamber equipped with a magnetic stirrer. Subsequently, the foil underwent irradiation from a laser beam, tracing a spiral pattern for fifteen minutes (see Fig. 4.1). Consistency in laser parameters, encompassing irradiation duration and pattern, was meticulously upheld throughout the experiments.

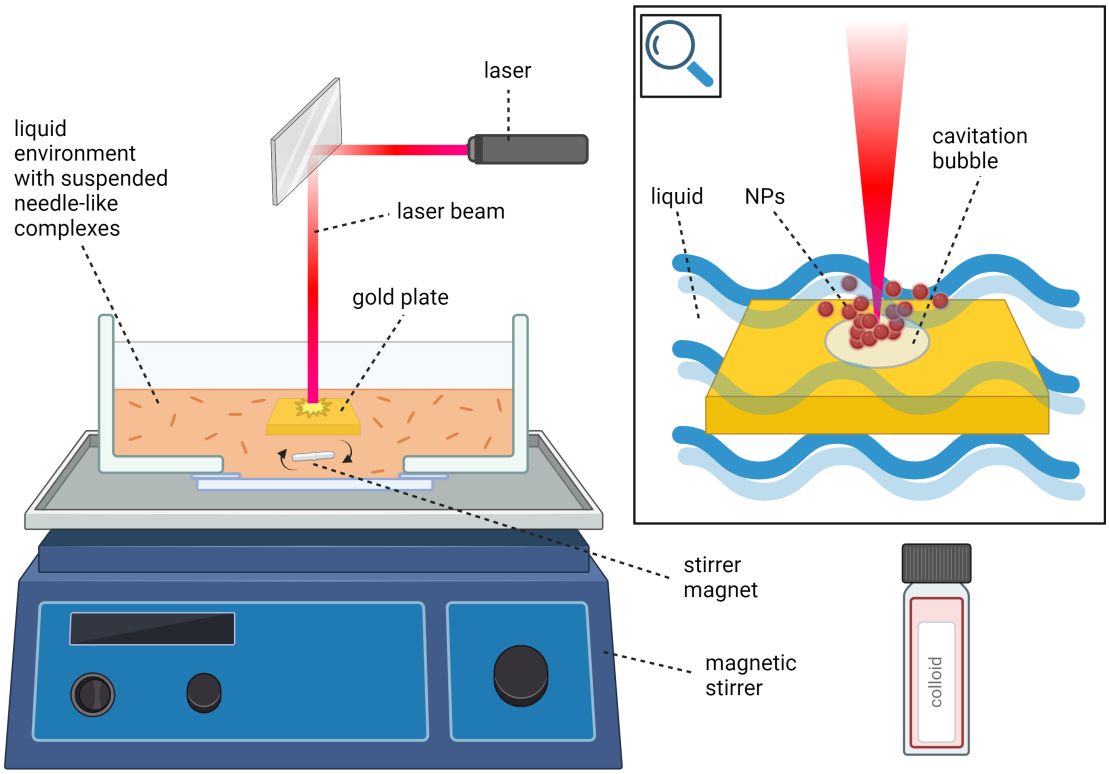

Figure 4.1: RLAL Schematic. The central focus of the diagram (left) delineates key experimental conditions, notably depicting the liquid housing precursor complexes and the precise positioning of the gold plate at the laser's focal length. The upper-right segment provides a broad overview of the NP creation process via RLAL. Meanwhile, the lower-right quadrant illustrates a tube containing the prepared colloidal solution.

In the initial phase of experimentation, the solid gold target was positioned at the focal point of the laser beam. Two trials were undertaken, varying solely in the concentration of the precursor within the RLAL medium. The first trial employed 0.1 ml of $KAuBr_4$ α-CD, while the second utilized 1 ml of the same solution. Given that the total ablation medium volume amounted to 40 ml, the remaining volume

was supplemented with demineralized H_2O. Consequently, the first experiment operated with a precursor concentration of 0.25 vol%, while the second was at 2.5 vol%. Despite these efforts, the outcomes proved unsatisfactory, indicating inadequacies in the RLAL parameters. Subsequent examination via SEM revealed likely disruptions of the complexes, including particle melting and subsequent fusion. In response to these findings, adjustments were implemented for the subsequent series of experiments. The primary objective was to attain lower temperatures and reduce laser intensity during ablation compared to those encountered at the focal point. As documented in existing literature, the placement of the target concerning the laser beam profoundly influences the intensity experienced at that specific location. Additionally, factors such as optical components and the inherent properties of the liquid medium significantly contribute to this phenomenon. Variations in energy intensity distribution and alterations in beam radius along the laser's trajectory are contingent upon the optical attributes of elements encountered. Identifying the precise focal point, potentially maximizing NP production, or in this context, pinpointing regions of diminished laser intensity is not an easy task. Often, a multifaceted and time-intensive approach is required for this endeavor [88].

After conducting a series of measurements aimed at assessing the impact of the target's position on RLAL (utilizing a gold foil immersed in pure H_2O), the subsequent target positions were selected:

- FOCAL POSITION (F)
  - to compare and track the influence of concentration
- MIDDLE POSITION (M): 0.71 cm above the focal plane
  - the threshold for visibly confirmed ablation
- HIGHEST POSITION (H): 0.9 cm above the focal plane
  - potentially suitable for the formation of smaller particles and clusters. Note that according to the latest computational simulations on LAL, it is believed that lower fluence values can enable the formation of small particles and clusters [89].

Three different volume concentrations of the precursor in the RLAL environment were also selected:

- 0.125 vol%: 50 μl
- 0.25 vol%: 100 μl
- 1.25 vol%: 500 μl

Subsequently, a comprehensive series of experiments encompassing all possible combinations of these settings was executed, totaling nine trials. Each prepared sample was meticulously labeled based on the utilized combination, employing the format: POSITION - VOLUME CONCENTRATION OF PRECURSOR (_SN if it was a supernatant). This systematic labeling approach facilitated seamless tracking of samples throughout the experimental process, ensuring clarity when correlating results with specific conditions. For instance, a sample denoted as F-0.25%_SN would signify a supernatant coming from irradiation at the focal position with a precursor volume concentration of 0.25%. This structured naming convention proved instrumental in streamlining the management and analysis of experimental data. Subsequently, the resulting colloidal solutions were consistently transferred into 40 ml test tubes for further processing (see Fig. 4.2).

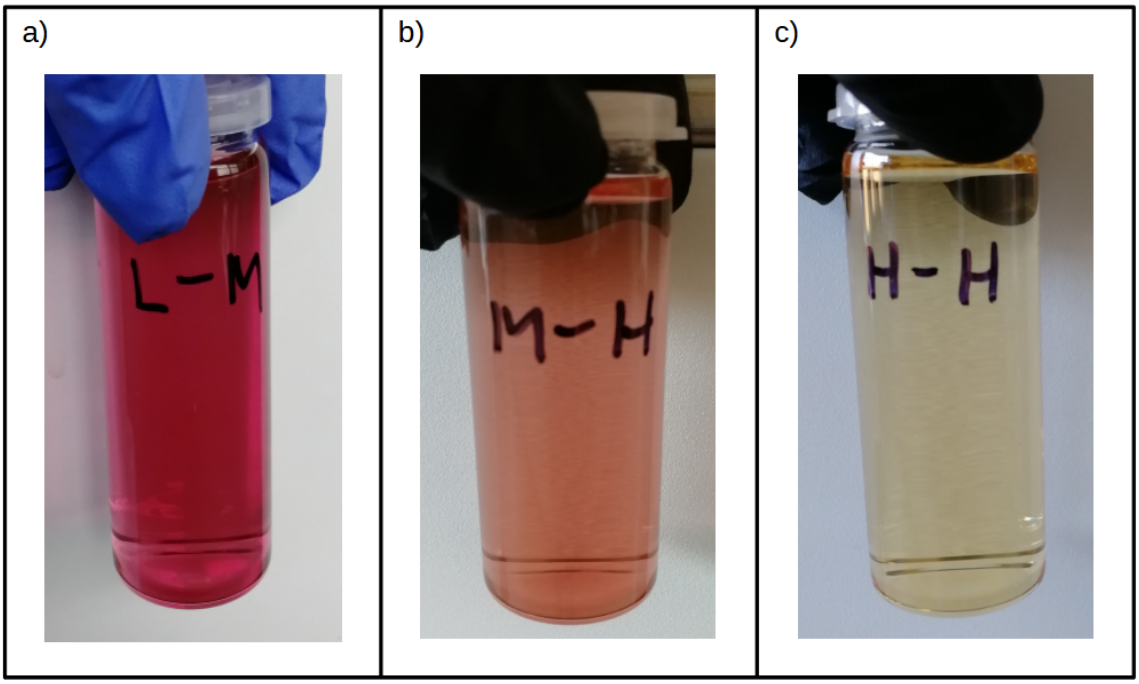

Figure 4.2: Examples of colloid solutions prepared by laser irradiation. a) Sample F-0.25%, b) sample M-1.25%, c) sample H-1.25%.

4.4 Laser parameters

For the synthesis process, we utilized the Onefive Origami XP-S, an advanced industrial femtosecond laser renowned for its high energy output. This laser boasts suitable specifications for our purposes, including a maximum average output power of 5.1 W, pulse lengths ranging from 200 fs to 400 fs, and a central wavelength of 1030 nm. With a maximum repetition frequency of 1 MHz and a single pulse energy capacity of up to 75 μJ, this laser operates at peak performance. Throughout the experiment, we leveraged these parameters at their maximum values to ensure optimal results.

4.5 Process of sample cleaning

The colloidal solutions, now laden with NPs, underwent a centrifuging process lasting fifteen minutes at 14,500 revolutions per minute (rpm) within 1.5 ml Eppendorf tubes, utilizing a MiniSpin plus centrifuge. This particular centrifuge, operating without cooling, is equipped with an F-45-12-11 rotor and functions at 230 V/50-60 Hz. During centrifuging, the NPs precipitated, forming a distinct sediment at the bottom of the tubes. This sediment, comprising the settled NPs, is commonly referred to as the sediment phase. Concurrently, the liquid situated above the sediment, known as the supernatant, harbors unreacted precursor residues and notably, floating particles generated during the ablation process. These floating particles, lacking sufficient mass or size, remain suspended in the liquid phase and do not settle. Subsequently, the supernatant was meticulously decanted from each sample, occasionally reserved for subsequent analytical procedures (see Fig. 4.3).

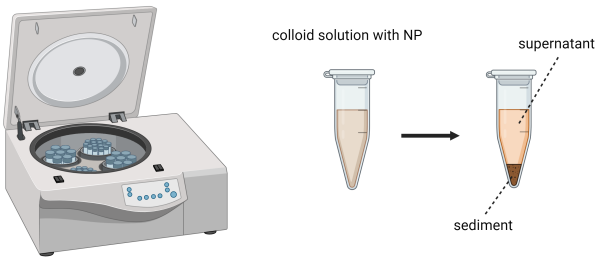

Figure 4.3: Visual depiction of the centrifuging process: An Eppendorf tube is carefully inserted into the centrifuge device. Following the centrifuging procedure, the resultant outcome reveals the distinct separation of sediment and supernatant within the tube.

The remaining sediment was carefully re-suspended in the colloidal solution, and the Eppendorf tubes were subjected to another round of centrifuging until all of the colloidal solution was completely depleted. Subsequently, upon removal of the supernatant from the last batch, the tubes were replenished with demineralized water (demiH_2O) and subjected to homogenization using an ultrasonic cleaner (SONOREX DIGITEC DT510H, operating at 35 kHz with a capacity of 9.7 liters), followed by another cycle of centrifuging. This iterative process was reiterated, with each cycle involving the transfer of the homogenized colloid between Eppendorf tubes to minimize their quantity. The cleaning procedure culminated in the consolidation of a single Eppendorf tube, theoretically containing the maximum amount of sediment achievable.

5 Results and discussion

This bachelor's thesis aimed to synthesize NPs with tailored shapes. The prepared samples underwent scrutiny through diverse analytical methods to ascertain the extent to which the desired shape modification of the NPs was achieved. This thorough analysis sought to gauge the efficacy of the experimental procedures in crafting NPs with distinct, non-standard geometries, diverging from the conventional spherical forms typically observed in gold NP synthesis.

5.1 Precursor complexes

Firstly, it is important to evaluate the initial preparation of the $KAuBr_4$ complexes with α-CDs, as this work originates from there. We successfully replicated the synthesis of these NPs according to the methodology of the original article [17]. Our efforts yielded consistent results, enabling us to reliably produce these complexes as precursors for subsequent experiments (see Fig. 5.1).

Figure 5.1: Photograph depicting the suspension of the $KAuBr_4$ complex with α-CD.

The success of synthesizing these specific complexes is corroborated by two characterization methods: scanning electron microscopy (SEM) (Figure 5.2) and nuclear magnetic resonance (NMR) (Figures 5.3, and 5.4). Both techniques validate the formation of nano-objects exhibiting needle-like shapes and structures.

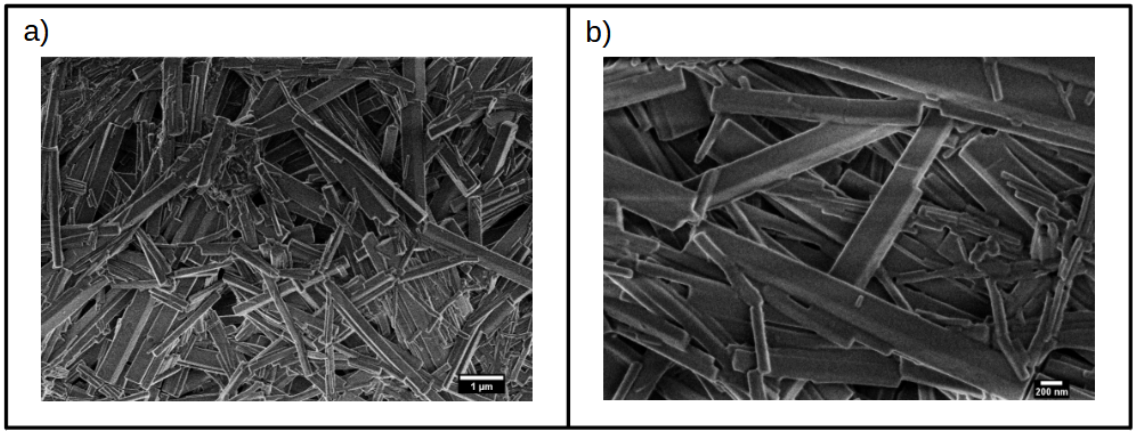

Figure 5.2: SEM images of $KAuBr_4$ with α-CD complex. a) General micrograph, b) zoomed-in micrograph.

The SEM micrographs vividly depict the emergence of elongated rectangular shapes, typically featuring dimensions where one dimension (length) extends to several micrometers, while the other two dimensions measure around one micrometer or less. These structural characteristics align precisely with the theoretically anticipated and targeted shapes established prior to chemical synthesis [17], which are 1D cable superstructures formed by alternately arranged $K(OH_2)_6{}^+$ and $AuBr_4{}^-$ in ionic conductors wrapped in α-CD toruses. CDs act as second-sphere ligands, with the cation and anion placed between their heads and tails in the structure. SEM is thereby analytically confirming the structure of the prepared complex.

As shown in Figures 5.3 and 5.4, in solid-state ^{13}C NMR spectra of α-CDs with gold, observed peaks exhibit notable upfield shifts compared to those of pure α-CDs. Peaks corresponding to C_1 (90-95 ppm), C_4 (66-75 ppm), $C_{2,3,5}$ (57-66 ppm), and C_6 (47-53 ppm) of CDs have all shifted by 8-11 ppm, alongside broadening [90, 91], indicative of significant interactions between Au ions with the CDs molecule, understood as successful Au adsorption by CDs in the original journal [17].

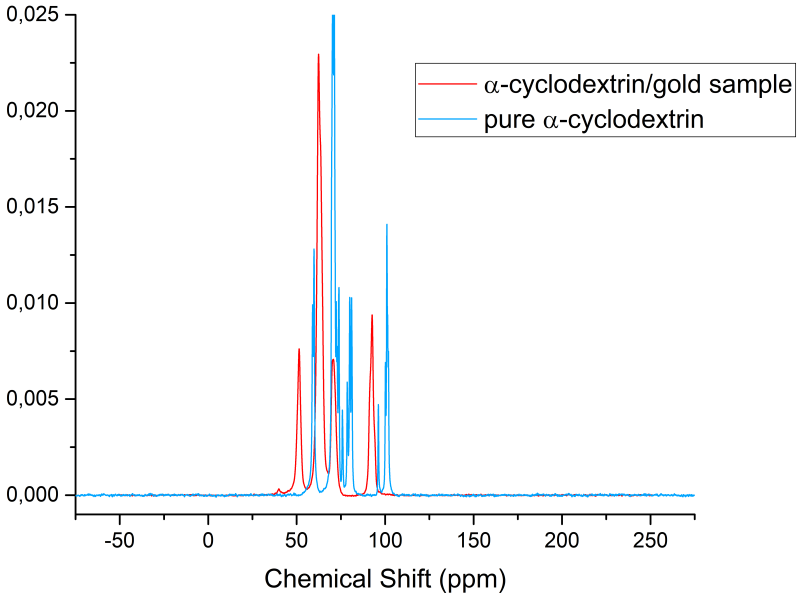

Figure 5.3: NMR Spectrum for precursor complex No.1: Cross-Polarization/Magic Angle Spinning (^{13}C CP/MAS) spectrum with high-powered ^{1}H decoupling, comparing pure $KAuBr_4$-CDs (blue) against the α-CDs/gold sample (red).

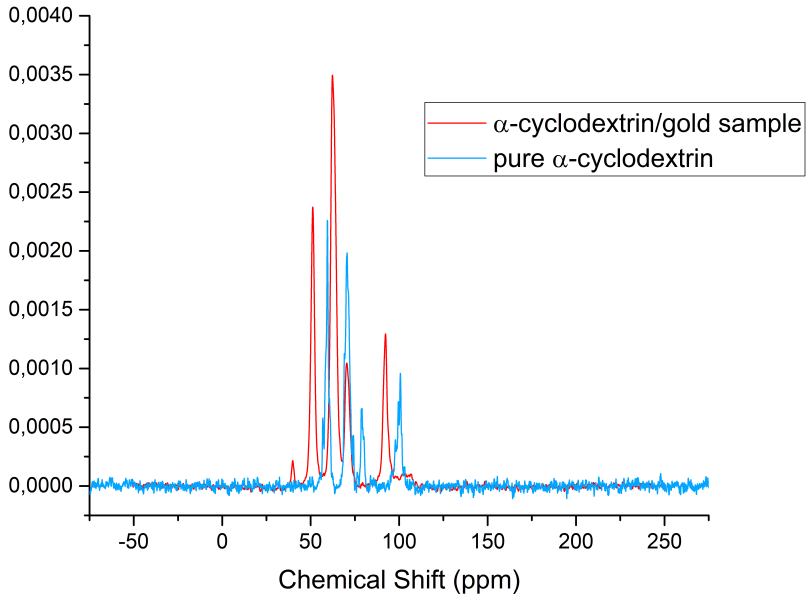

Figure 5.4: NMR Spectrum for precursor complex No.2: Hahn Echo ^{13}C spectrum (with high-powered ^{1}H decoupling), showcasing pure α-CDs (blue) alongside the α-CDs/gold sample (red).

5.2 Absorbance by UV-Vis Spectroscopy

UV-Vis spectroscopy was employed to measure the absorbance of all 9 (or 18, including the supernatants) prepared samples (see Fig. 5.5). In nearly all displayed dependencies, a prominent peak around 540 nm was consistently observed, corresponding to the absorbance typically associated with spherical gold NPs. However, in one distinct case, a peak emerged around 390 nm, aligning with the absorbance characteristic of the precursor complexes (needle-like $KAuBr_4$ with α-CD) before laser irradiation.

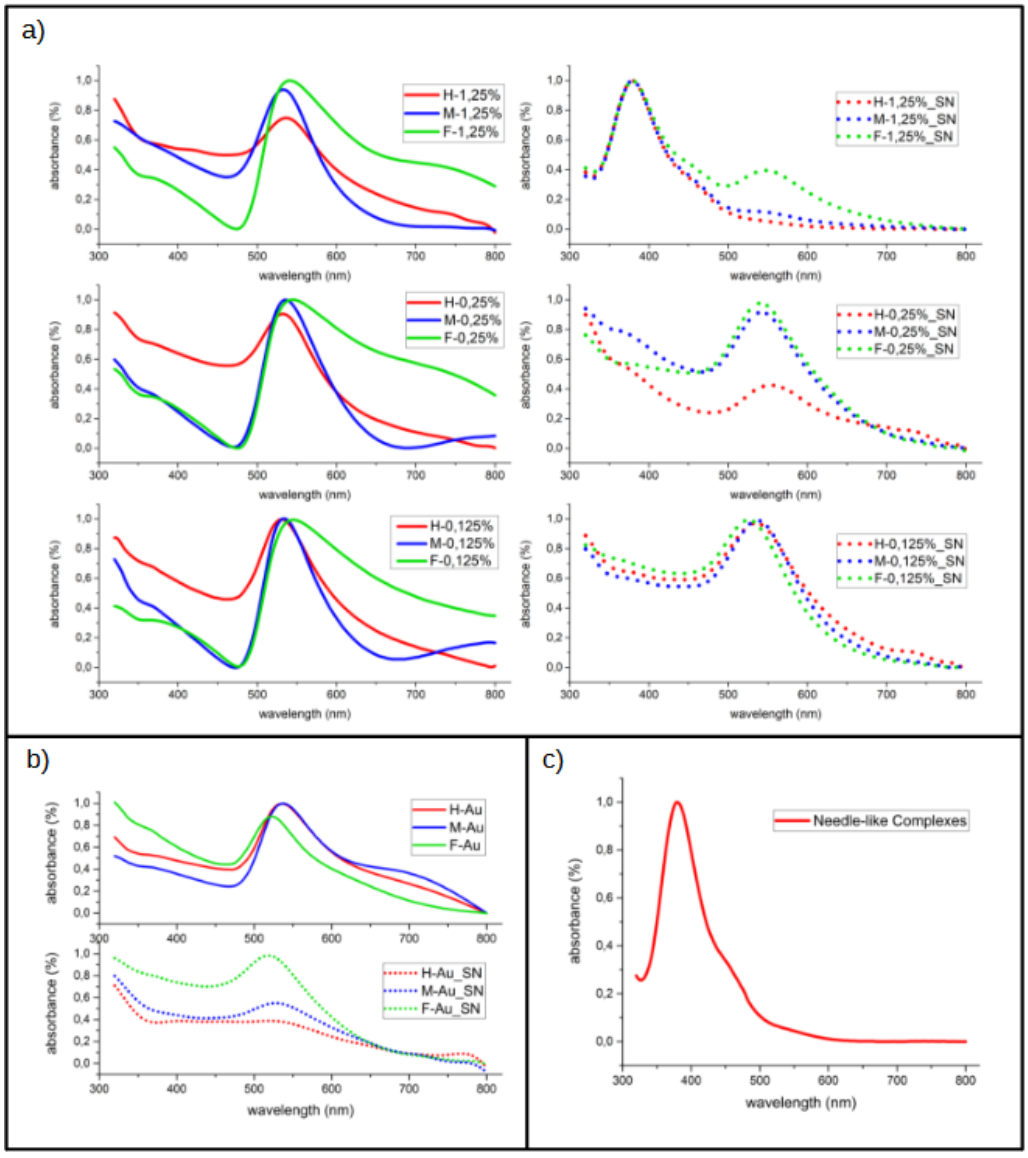

Figure 5.5: Absorbance by UV-Vis spectroscopy. a) Absorbance of all laser-synthesized samples, b) samples synthesized without the presence of the complex precursors, and c) precursor complex.

Across all absorbance measurements of the samples, a sharp peak is consistently observed, aligning with spherical gold NPs in eight out of nine cases. However, the graphs also reveal additional peaks or at least differences compared to the measurements of gold particles alone without the colloidal precursor, although these do not reach as pronounced values. Nevertheless, these observations suggest potential alterations in the shape of the prepared particles. According to the Mie theory [92], the emergence of additional peaks signifies a transition from a spherical to a more angular form, where sharper edges exhibit heightened SPR. Such variations may also manifest in absorbance measurements of particles within a homogenized colloidal solution.

5.3 SEM

All samples prepared via the RLAL method underwent subsequent imaging using SEM. These images capture both the nine sediment samples and their corresponding supernatants.

The bright objects evident in these images, indicative of their metallic (i.e., gold) composition, predominantly exhibit a spherical morphology (see Fig. 5.6). Occasionally, structures emerge, likely agglomerations of spherical particles forming non-spherical shapes. The gray material observed in many images represents the organic constituents of the samples, specifically CDs or their remnants. It appears that the organic component often underwent degradation due to the intense laser irradiation, unable to absorb such substantial energy. Consequently, the reaction temperature escalated, occasionally resulting in the melting or complete degradation of the organic material. Nonetheless, among the images, there are instances confirming the formation of non-spherical particles with angular features. Of particular interest are images primarily derived from the supernatants (see Fig. 5.7). This observation suggests that the smallest particles generated (floating within the colloid), which were unable to settle into the sediment, exhibited a greater propensity to adopt diverse shapes. Although the small particles produced by RLAL, typically around 5 nm and 60 nm in size (RLAL produces NPs with a bimodal size distribution) [89], are not comparable to the size of Au ions, they are more prone to undergo adsorption by α-CDs. Aided by CDs' capacity to form non-spherical structures due to their second-sphere coordination capabilities, angular NPs can be produced. However, it is crucial to note that more conclusive assessments would require examining the samples at a higher resolution than was feasible to confirm with the employed instruments, thus, the angularity of the shapes in intriguing and promising specimens could lead to more impactful endeavors.

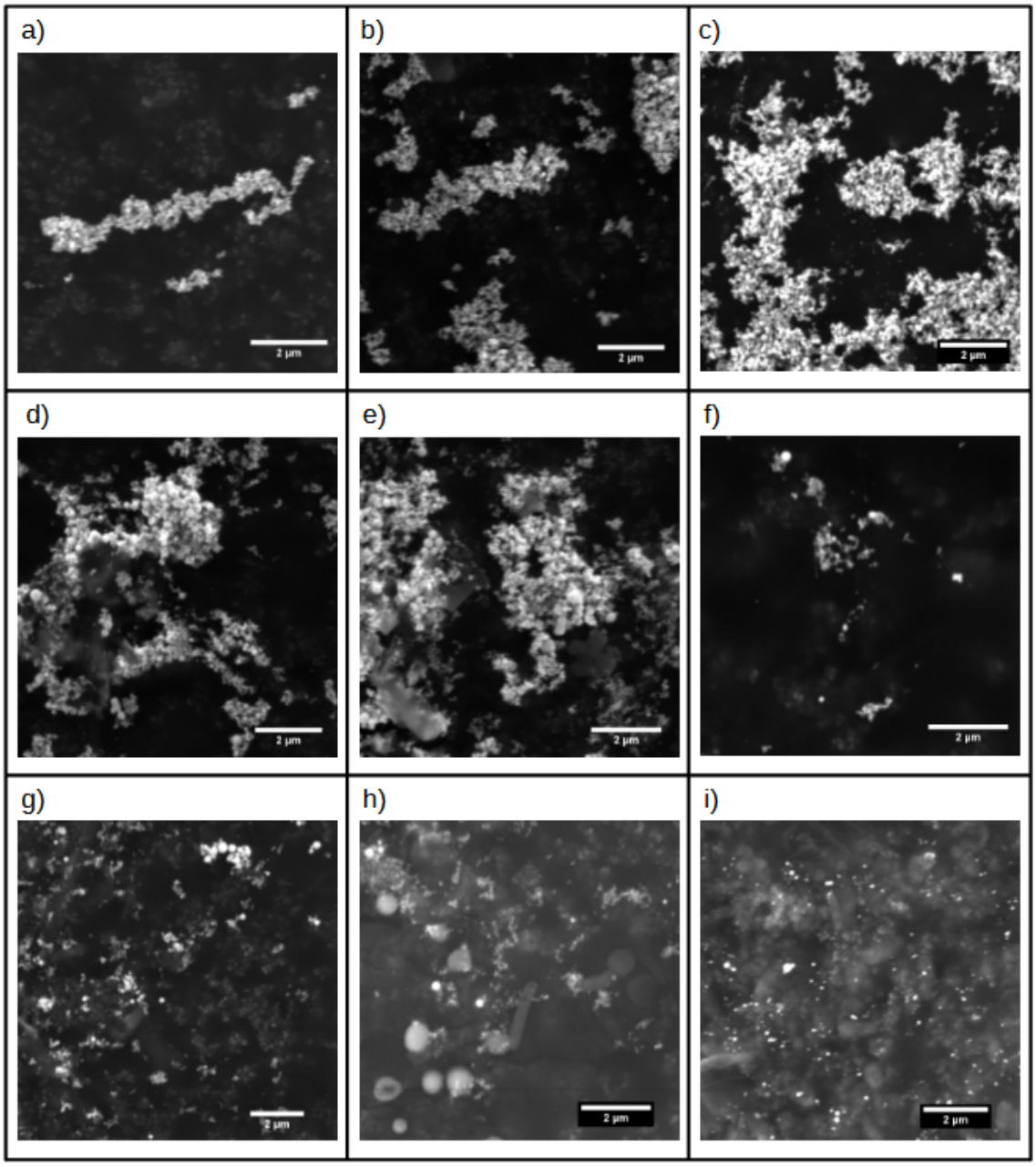

Figure 5.6: SEM images of the sediments. a) Sample F-0.125%, b) F-0.25%, c) F-1.25%, d) M-0.125%, e) M-0.25%, f) M-1.25%, g) H-0.125%, h) H-0.25%, and i) H-1.25%.

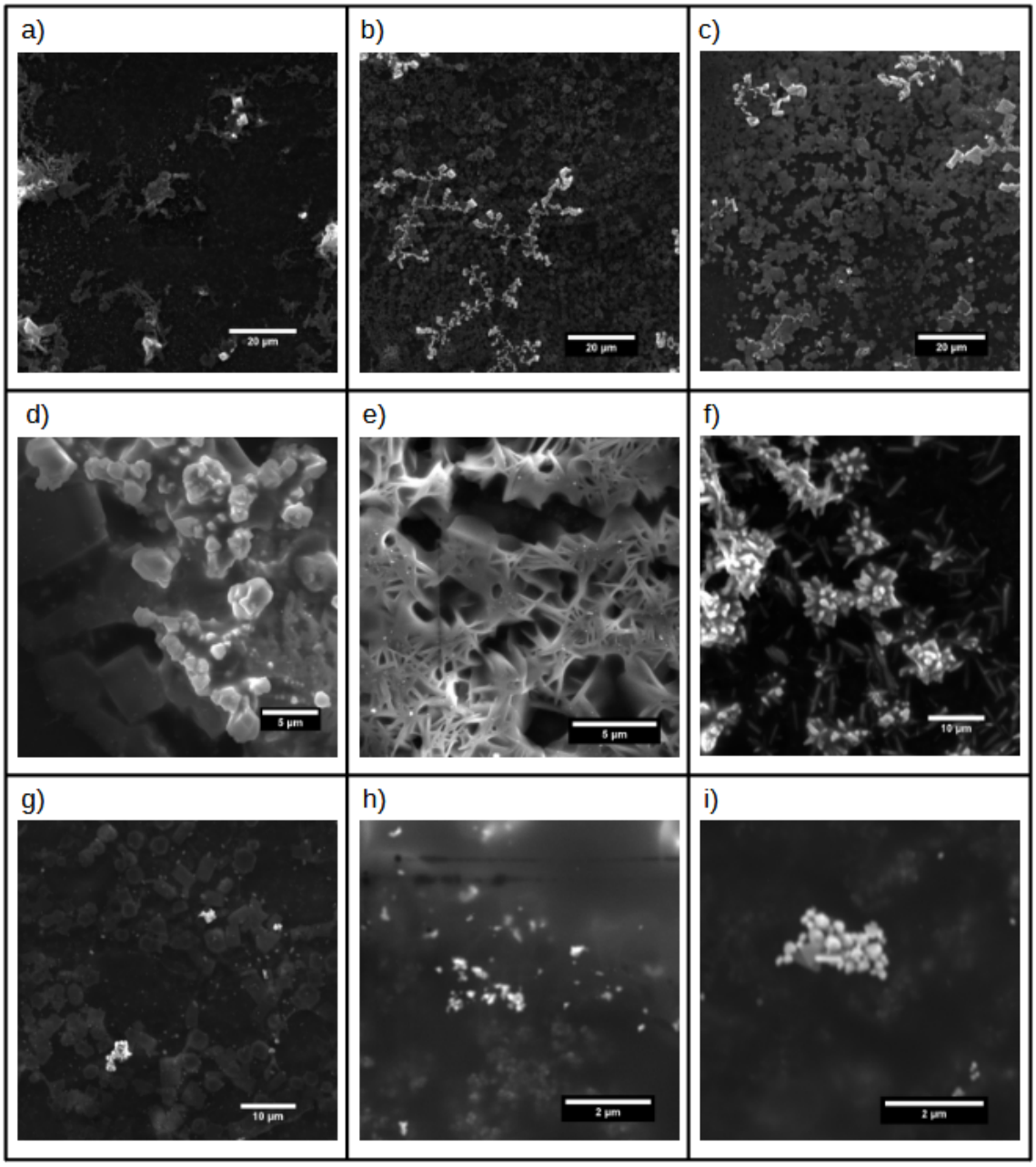

Figure 5.7: SEM images of the supernatants. a) Sample F-0.125%_SN, b) F-0.25%_SN, c) F-1.25%_SN, d) M-0.125%_SN, e) M-0.25%_SN, f) M-1.25%_SN, g) H-0.125%_SN, h) H-0.25%_SN, and i) H-1.25%_SN.

The samples displaying the most significant morphological modifications were selected as the most promising in pursuit of creating NPs of different shapes than the typical spherical gold NPs (see Fig. 5.8).

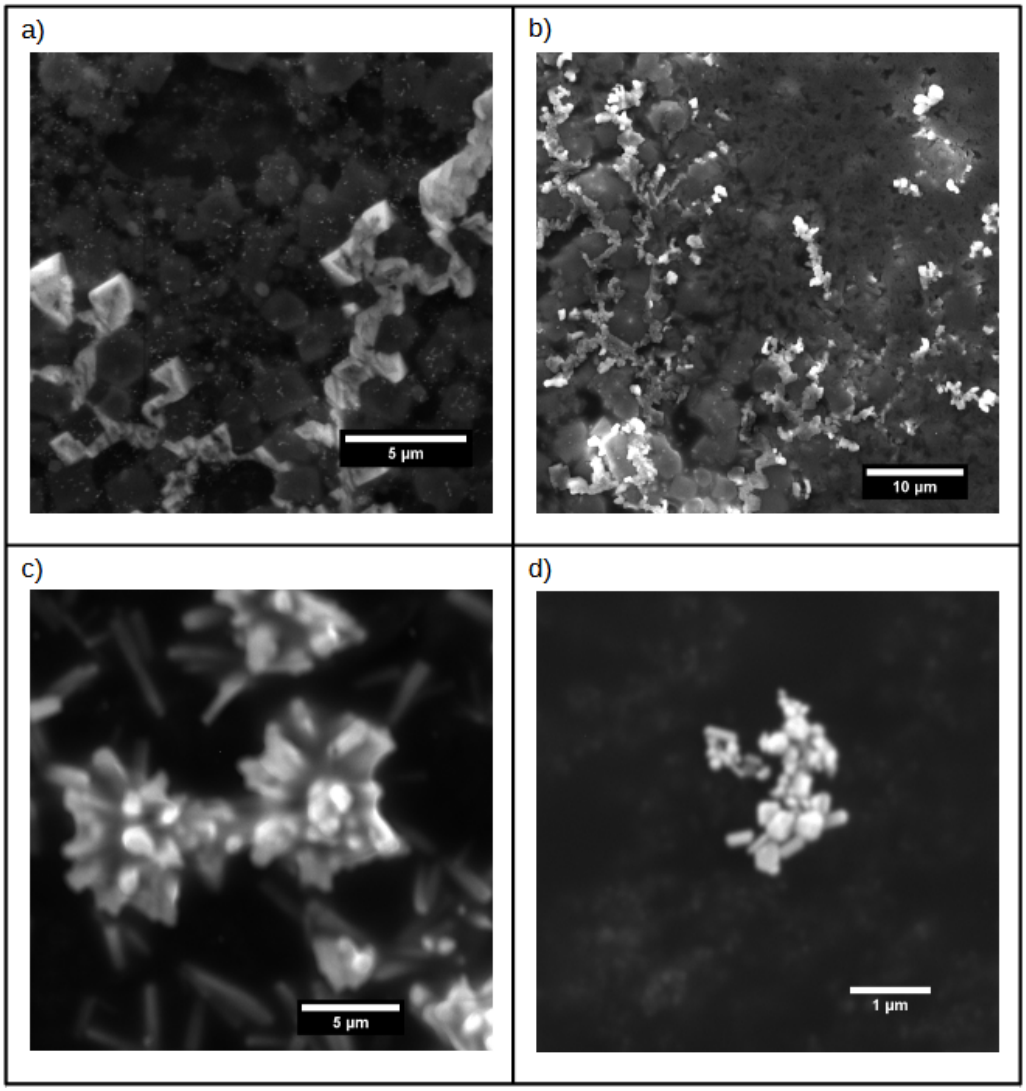

Figure 5.8: Additional SEM images of promising samples for the modified shape of NPs. a) Sample F-0.25%_SN, b) F-1.25%_SN, c) M-1.25%_SN, and d) H-1.25%_SN.

5.4 Stability by UV-Vis Spectroscopy

Regarding samples showing promising alterations in particle shapes, a stability analysis was performed, involving the measurement of time-dependent absorbance changes over an eight-day period, with intensive measurements conducted on the first day (see Fig. 5.9). Generally, the results indicated that samples in colloidal form exhibited limited stability. Absorbance was consistently measured at specific predetermined wavelengths derived from previous analyses of all samples. According to the study reported in Ref. [93] a wavelength of 400 nm was chosen for the sediments, while for three of the four supernatants, a wavelength of 330 nm was selected to correspond with the valley position in the absorbance wavelength dependencies. However, for sample F-0.25%_SN, where no valley was present at this wavelength, 450 nm was chosen, where a small valley was observed.

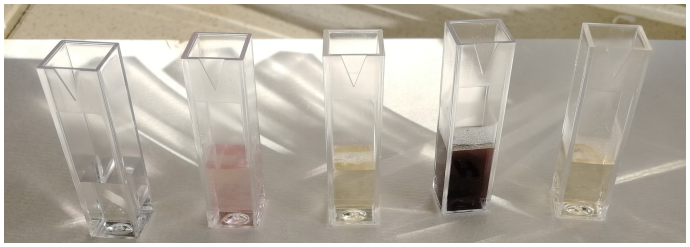

Figure 5.9: Photograph of prepared colloid solutions in plastic cuvettes during stability analysis using UV-Vis spectrometer.

Among the sediments, sample M-1.25% emerged as the most stable, with its initial absorbance value decreasing only slightly over approximately 8.5 hours. Conversely, the sample F-0.25% exhibited the most rapid decline in absorbance values. The decreasing trend across all dependencies suggests particle settling from the initially homogeneous colloidal solution. This settling could be attributed to the size and weight of the particles themselves or to the phenomenon of agglomeration, where individual particles cluster together, increasing mass and initiating settling.

Supernatants appeared relatively more stable due to these reasons; however, the technical parameters of the measuring instrument, particularly its measurement inaccuracy, require careful consideration in their case. Error bars are included in the graphs, derived from the technical specifications of the spectrometer used. According to the manufacturer, for measured absorbance units up to 0.5, the measurement inaccuracy is a fixed value of 5 mAbs. For measured absorbance values from 0.5 to 2, the inaccuracy is 1% of the measured value. The instrument's measurement inaccuracy significantly impacts the supernatants, given their relatively low measured absorbance values. Thus, it is evident from the graphs that these results must be interpreted with considerable caution. Notably, significant error bars are also observed for one of the sediments, specifically sample H-1.25% (see Fig. 5.10).

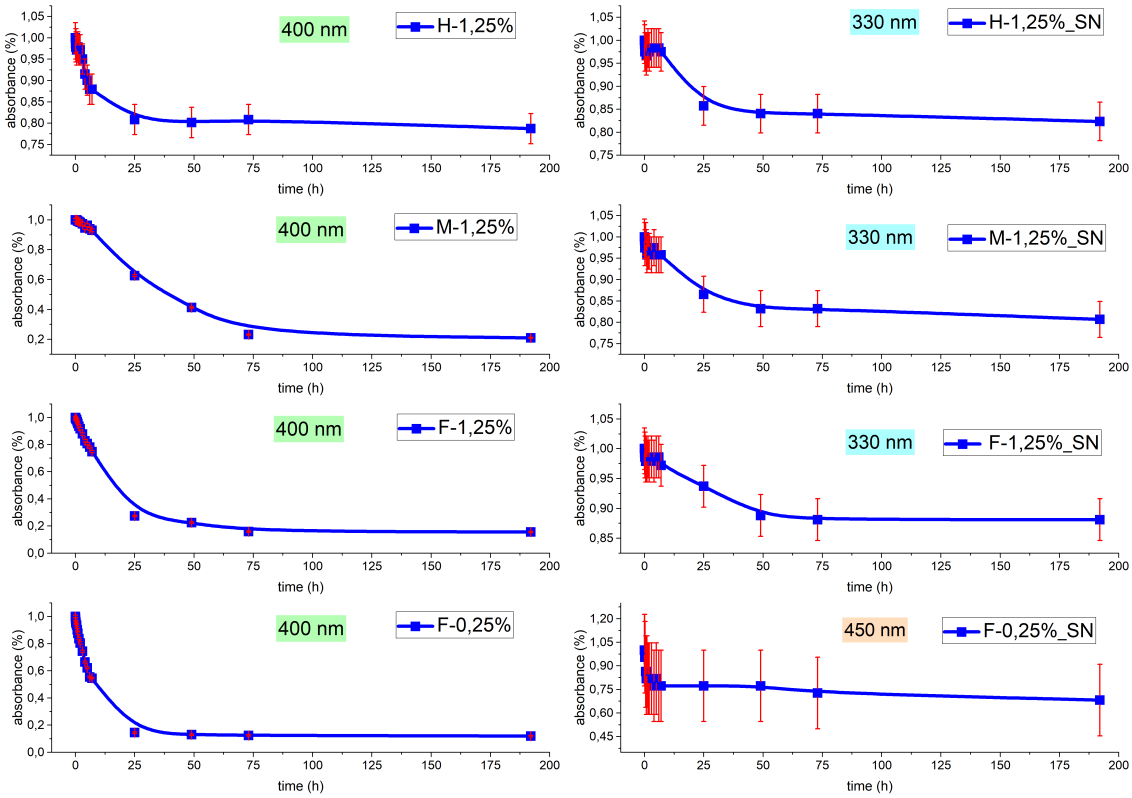

Figure 5.10: Stability by UV-Vis Spectroscopy.

6 Conclusion

In this bachelor's thesis, non-spherical NPs were successfully synthesized by RLAL, taking as a liquid environment a complex formed by the controlled adsorption of $KAuBr_4$ by α-CDs, initially shaped like needles. Confirmation of this complex was assessed by NMR and SEM analyses.

Our driving hypothesis for synthesizing the non-spherical NPs was that during the RLAL process, the complex acted as a growth director to create NPs of different shapes than the typically formed spherical gold NPs in pure water environments. Initial experiments revealed that the laser intensity at the focus was too high, degrading the organic components of the precursors. It was also determined that the synthesis should aim to create smaller NPs or clusters capable of being adsorbed by the complexes to grow into the intended shapes. Thus, the gold solid target was positioned above the focal point to irradiate the sample at a low fluence, where conditions for creating the desired NPs were more favorable.

In the subsequent part, NPs were synthesized at three different positions of the gold target and with three different complex concentrations. Two positions above the focal plane, specifically 0.71 cm and 0.9 cm above the focal plane, were chosen where lower laser intensity was presumed, and the third position was the focal point itself. Three concentrations of precursors (complexes) in the RLAL liquid environment were also set—0.125 vol%, 0.25 vol%, and 1.25 vol%—to observe the influence of the presence of complexes on the creation of specific NPs. All prepared samples were purified and then analyzed using UV-Vis spectroscopy and SEM. Absorbance measurements confirmed the predominant presence of spherical gold NPs but also suggested the existence of more angular shapes. The most interesting samples were supernatants, likely because they contained smaller-sized particles, which could have more likely undergone growth and interaction with the precursor complexes. Such smaller particles could have been adsorbed and further arranged in non-spherical shapes due to CD's second-sphere coordination capabilities. Stability analysis were conducted on the most promising samples; the supernatants H-1,25%S_N, M-1,25%_SN, F-1,25%_SN, F-0,25%_SN, and corresponding sediments H-1,25%, M-1,25%, F-1,25%, F-0,25%. It was found that none of the samples exhibited significant stability over time, with the most stable of the sediments being capable of withstanding unaltered for 8.5 hours. Supernatants, on the other hand, showed longer stability, but the measurement results were relatively influ-

enced by the technical inaccuracy (in low values of concentration) of the employed spectrometer.

In conclusion, it was proven with the help of UV-Vis and SEM micrograph analysis that NPs with non-spherical shapes were successfully synthesized, although not in large quantities and still simultaneously with spherical NPs. The most promising results were shown by the supernatant samples, indicating that smaller floating particles should be the focus of interest in future studies. Future directions may involve subjecting only the gold NPs from RLAL to laser fragmentation or melting and subsequently adding complexes as growth directors to create modified-shaped NPs, potentially even clusters.

References

[1] YANG, Minzheng; GUO, Mengfan; XU, Erxiang; REN, Weibin; WANG, Danyang; LI, Sean; ZHANG, Shujun; NAN, Ce-Wen; SHEN, Yang. Polymer nanocomposite dielectrics for capacitive energy storage. *Nature Nanotechnology*. 2024. ISSN 1748-3395. Available from DOI: 10.1038/s41565-023-01541-w.

[2] WYRZYKOWSKA, Ewelina et al. Representing and describing nanomaterials in predictive nanoinformatics. *Nature Nanotechnology*. 2022, vol. 17, no. 9, pp. 924–932. ISSN 1748-3395. Available from DOI: 10.1038/s41565-022-01173-6.

[3] ANU MARY EALIA, S; SARAVANAKUMAR, M P. A review on the classification, characterisation, synthesis of nanoparticles and their application. *IOP Conference Series: Materials Science and Engineering* [online]. 2017, vol. 263, pp. 032019 [visited on 2024-02-09]. ISSN 1757-8981. Available from DOI: 10.1088/1757-899X/263/3/032019.

[4] ZHANG, L; GU, Fx; CHAN, Jm; WANG, Az; LANGER, Rs; FAROKHZAD, Oc. Nanoparticles in Medicine: Therapeutic Applications and Developments. *Clinical Pharmacology & Therapeutics* [online]. 2008, vol. 83, no. 5, pp. 761–769 [visited on 2024-05-10]. ISSN 0009-9236. Available from DOI: 10.1038/sj.clpt.6100400.

[5] ABID, Namra et al. Synthesis of nanomaterials using various top-down and bottom-up approaches, influencing factors, advantages, and disadvantages: A review. *Advances in Colloid and Interface Science* [online]. 2022, vol. 300, pp. 102597 [visited on 2023-12-08]. ISSN 0001-8686. Available from DOI: 10.1016/j.cis.2021.102597.

[6] *Synthesis of nanomaterials using top-down methods - ScienceDirect* [online] [visited on 2023-12-08]. Available from: https://www.sciencedirect.com/science/article/abs/pii/B9780323998772000072.

[7] GU, Hongyan; ZHANG, Junwei; FAUCHER, Santiago; ZHU, Shiping. Controlled chattering—a new 'cutting-edge' technology for nanofabrication. *Nanotechnology* [online]. 2010, vol. 21, no. 35, pp. 355302 [visited on 2023-12-08]. ISSN 0957-4484. Available from DOI: 10.1088/0957-4484/21/35/355302.

[8] *Plasmonic Properties of Anchored Nanoparticles Fabricated by Reactive Ion Etching and Nanosphere Lithography | The Journal of Physical Chemistry C* [online] [visited on 2023-12-08]. Available from: https://pubs.acs.org/doi/abs/10.1021/jp064094w.

[9] *Nanomaterials Synthesis Methods - Metrology and Standardization of Nanotechnology - Wiley Online Library* [online] [visited on 2023-12-08]. Available from: https://onlinelibrary.wiley.com/doi/10.1002/9783527800308.ch4.

[10] *Chemical precipitation | Water Treatment, pH Adjustment & Coagulation | Britannica* [online]. 2023 [visited on 2023-11-13]. Available from: https://www.britannica.com/science/chemical-precipitation.

[11] BARCIKOWSKI, Stephan; AMENDOLA, Vincenzo; LAU, Marcus; MARZUN, Galina; REHBOCK, Christoph; REICHENBERGER, Sven; ZHANG, Dongshi; GÖKCE, Bilal. *Handbook of Laser Synthesis & Processing of Colloids* [online]. In collab. with DUEPUBLICO: DUISBURG-ESSEN PUBLICATIONS ONLINE, University Of Duisburg-Essen. DuEPublico: Duisburg-Essen Publications online, University of Duisburg-Essen, Germany, 2019 [visited on 2023-11-13]. Available from DOI: 10.17185/DUEPUBLICO/70584.

[12] FRIAS BATISTA, Laysa M.; NAG, Ashish; MEADER, Victoria K.; TIBBETTS, Katharine Moore. Generation of nanomaterials by reactive laser-synthesis in liquid. *Science China Physics, Mechanics & Astronomy* [online]. 2022, vol. 65, no. 7, pp. 274202 [visited on 2023-11-13]. ISSN 1869-1927. Available from DOI: 10.1007/s11433-021-1835-x.

[13] MARKS, L D; PENG, L. Nanoparticle shape, thermodynamics and kinetics. *Journal of Physics: Condensed Matter* [online]. 2016, vol. 28, no. 5, pp. 053001 [visited on 2024-05-02]. ISSN 0953-8984. Available from DOI: 10.1088/0953-8984/28/5/053001.

[14] LU, Yunfeng; FAN, Hongyou; STUMP, Aaron; WARD, Timothy L.; RIEKER, Thomas; BRINKER, C. Jeffrey. Aerosol-assisted self-assembly of mesostructured spherical nanoparticles. *Nature*. 1999, vol. 398, no. 6724, pp. 223–226. ISSN 1476-4687. Available from DOI: 10.1038/18410.

[15] JIA, Chuancheng; LIN, Zhaoyang; HUANG, Yu; DUAN, Xiangfeng. Nanowire Electronics: From Nanoscale to Macroscale. *Chemical Reviews* [online]. 2019, vol. 119, no. 15, pp. 9074–9135 [visited on 2024-05-10]. ISSN 0009-2665. Available from DOI: 10.1021/acs.chemrev.9b00164.

[16] HAROON ANWAR, Saad. A Brief Review on Nanoparticles: Types of Platforms, Biological Synthesis and Applications. *Research & Reviews Journal of Material Sciences* [online]. 2018, vol. 06, no. 02 [visited on 2024-05-10]. ISSN 23216212. Available from DOI: 10.4172/2321-6212.1000222.

[17] LIU, Zhichang; SAMANTA, Avik; LEI, Juying; SUN, Junling; WANG, Yuping; STODDART, J Fraser. Cation-Dependent Gold Recovery with α-Cyclodextrin Facilitated by Second-Sphere Coordination. *Journal of the American Chemical Society*. Available from DOI: 10.1021/jacs.6b04986.

[18] LIU, Zhichang et al. Selective isolation of gold facilitated by second-sphere coordination with -cyclodextrin. *Nature Communications* [online]. 2013, vol. 4, no. 1, pp. 1855 [visited on 2023-11-13]. ISSN 2041-1723. Available from DOI: 10.1038/ncomms2891.

[19] LIU, Wenqi; JONES, Leighton O.; WU, Huang; STERN, Charlotte L.; SPONENBURG, Rebecca A.; SCHATZ, George C.; STODDART, J. Fraser. Supramolecular Gold Stripping from Activated Carbon Using -Cyclodextrin. *Journal of the American Chemical Society* [online]. 2021, vol. 143, no. 4, pp. 1984–1992 [visited on 2023-11-13]. ISSN 0002-7863. Available from DOI: 10.1021/jacs.0c11769.

[20] FINDIK, Fehim. Nanomaterials and their applications. 2021, vol. 9, no. 3. Available from DOI: 10.21533/pen.v9i3.1837.

[21] FEYNMAN, Richard P. Plenty of Room at the Bottom. Available from DOI: CaltechES:23.5.1960Bottom.

[22] RODUNER, Emil. Size matters: why nanomaterials are different. *Chemical Society Reviews* [online]. 2006, vol. 35, no. 7, pp. 583 [visited on 2024-02-07]. ISSN 0306-0012. Available from DOI: 10.1039/b502142c.

[23] SHAJI, Ashin; ZACHARIAH, Ajesh K. Chapter 9 - Surface Area Analysis of Nanomaterials. In: THOMAS, Sabu; THOMAS, Raju; ZACHARIAH, Ajesh K.; MISHRA, Raghvendra Kumar (eds.). *Thermal and Rheological Measurement Techniques for Nanomaterials Characterization*. Elsevier, 2017, pp. 197–231. Micro and Nano Technologies. ISBN 978-0-323-46139-9. Available from DOI: https://doi.org/10.1016/B978-0-323-46139-9.00009-8.

[24] MEKUYE, Bawoke; ABERA, Birhanu. Nanomaterials: An overview of synthesis, classification, characterization, and applications. *Nano Select* [online]. 2023, vol. 4, no. 8, pp. 486–501 [visited on 2024-03-05]. ISSN 2688-4011. Available from DOI: 10.1002/nano.202300038.

[25] DAS, B. B.; MITRA, Arkadeep. Nanomaterials for Construction Engineering-A Review. *International Journal of Materials, Mechanics and Manufacturing* [online]. 2014, pp. 41–46 [visited on 2024-05-10]. ISSN 17938198. Available from DOI: 10.7763/IJMMM.2014.V2.96.

[26] ZHANG, Xi-Feng; LIU, Zhi-Guo; SHEN, Wei; GURUNATHAN, Sangiliyandi. Silver Nanoparticles: Synthesis, Characterization, Properties, Applications, and Therapeutic Approaches. *International Journal of Molecular Sciences* [online]. 2016, vol. 17, no. 9, pp. 1534 [visited on 2024-03-06]. ISSN 1422-0067. Available from DOI: 10.3390/ijms17091534.

[27] KOLAHALAM, Lalitha A.; KASI VISWANATH, I.V.; DIWAKAR, Bhagavathula S.; GOVINDH, B.; REDDY, Venu; MURTHY, Y.L.N. Review on nanomaterials: Synthesis and applications. *Materials Today: Proceedings* [online]. 2019, vol. 18, pp. 2182–2190 [visited on 2024-03-06]. ISSN 22147853. Available from DOI: 10.1016/j.matpr.2019.07.371.

[28] SMIJS, Threes; PAVEL. Titanium dioxide and zinc oxide nanoparticles in sunscreens: focus on their safety and effectiveness. *Nanotechnology, Science and Applications* [online]. 2011, pp. 95 [visited on 2024-02-11]. ISSN 1177-8903. Available from DOI: 10.2147/NSA.S19419.

[29] LI, Jinghong; ZHANG, Jin Z. Optical properties and applications of hybrid semiconductor nanomaterials. *Coordination Chemistry Reviews* [online]. 2009, vol. 253, no. 23, pp. 3015–3041 [visited on 2024-03-06]. ISSN 00108545. Available from DOI: 10.1016/j.ccr.2009.07.017.

[30] SRIDHARAN, Rajalakshmi; MONISHA, B.; KUMAR, P. Senthil; GAYATHRI, K. Veena. Carbon nanomaterials and its applications in pharmaceuticals: A brief review. *Chemosphere* [online]. 2022, vol. 294, pp. 133731 [visited on 2024-03-06]. ISSN 00456535. Available from DOI: 10.1016/j.chemosphere.2022.133731.

[31] KHARE, Rupesh; BOSE, Suryasarathi. Carbon Nanotube Based Composites-A Review. *Journal of Minerals and Materials Characterization and Engineering* [online]. 2005, vol. 04, no. 1, pp. 31–46 [visited on 2024-03-06]. ISSN 2327-4077. Available from DOI: 10.4236/jmmce.2005.41004.

[32] WU, Yanqing; FARMER, Damon B.; XIA, Fengnian; AVOURIS, Phaedon. Graphene Electronics: Materials, Devices, and Circuits. *Proceedings of the IEEE* [online]. 2013, vol. 101, no. 7, pp. 1620–1637 [visited on 2024-03-06]. ISSN 0018-9219. Available from DOI: 10.1109/JPROC.2013.2260311.

[33] FACCINI, Mirko; BORJA, Guadalupe; BOERRIGTER, Marcel; MORILLO MARTÍN, Diego; MARTÌNEZ CRESPIERA, Sandra; VÁZQUEZ-CAMPOS, Socorro; AUBOUY, Laurent; AMANTIA, David. Electrospun Carbon Nanofiber Membranes for Filtration of Nanoparticles from Water. *Journal of Nanomaterials* [online]. 2015, vol. 2015, pp. 1–9 [visited on 2024-03-06]. ISSN 1687-4110. Available from DOI: 10.1155/2015/247471.

[34] ARDUINI, Fabiana; CINTI, Stefano; MAZZARACCHIO, Vincenzo; SCOGNAMIGLIO, Viviana; AMINE, Aziz; MOSCONE, Danila. Carbon black as an outstanding and affordable nanomaterial for electrochemical (bio)sensor design. *Biosensors and Bioelectronics* [online]. 2020, vol. 156, pp. 112033 [visited on 2024-05-10]. ISSN 09565663. Available from DOI: 10.1016/j.bios.2020.112033.

[35] SAHAY, Rahul; REDDY, Venugopal Jayarama; RAMAKRISHNA, Seeram. Synthesis and applications of multifunctional composite nanomaterials. *International Journal of Mechanical and Materials Engineering* [online]. 2014, vol. 9, no. 1, pp. 25 [visited on 2024-03-06]. ISSN 1823-0334. Available from DOI: 10.1186/s40712-014-0025-4.

[36] KAPADIA, Chintan H.; MELAMED, Jilian R.; DAY, Emily S. Spherical Nucleic Acid Nanoparticles: Therapeutic Potential. *BioDrugs* [online]. 2018, vol. 32, no. 4, pp. 297–309 [visited on 2024-05-10]. ISSN 1173-8804. Available from DOI: 10.1007/s40259-018-0290-5.

[37] WANG, Chuan; TAKEI, Kuniharu; TAKAHASHI, Toshitake; JAVEY, Ali. Carbon nanotube electronics – moving forward. *Chem. Soc. Rev.* 2013, vol. 42, no. 7, pp. 2592–2609. Available from DOI: 10.1039/C2CS35325C.

[38] GUERRERO-MARTÍNEZ, Andrés; BARBOSA, Silvia; PASTORIZA-SANTOS, Isabel; LIZ-MARZÁN, Luis M. Nanostars shine bright for you. *Current Opinion in Colloid & Interface Science* [online]. 2011, vol. 16, no. 2, pp. 118–127 [visited on 2024-05-10]. ISSN 13590294. Available from DOI: 10.1016/j.cocis.2010.12.007.

[39] QIU, Xuefeng; CAO, Kai; LIN, Tingsheng; CHEN, Wei; YUAN, Ahu; WU, Jinhui; HU, Yiqiao; GUO, Hongqian. Drug delivery system based on dendritic nanoparticles for enhancement of intravesical instillation. *International Journal of Nanomedicine* [online]. 2017, vol. Volume 12, pp. 7365–7374 [visited on 2024-05-10]. ISSN 1178-2013. Available from DOI: 10.2147/IJN.S140111.

[40] HERMANN, Klaus E. Nanoparticles with cubic symmetry: classification of polyhedral shapes. *Journal of Physics: Condensed Matter* [online]. 2024, vol. 36, no. 4, pp. 045303 [visited on 2024-05-10]. ISSN 0953-8984. Available from DOI: 10.1088/1361-648X/ad0191.

[41] WU, Zhaohui; YANG, Shuanglei; WU, Wei. Shape control of inorganic nanoparticles from solution. *Nanoscale* [online]. 2016, vol. 8, no. 3, pp. 1237–1259 [visited on 2024-05-02]. ISSN 2040-3364. Available from DOI: 10.1039/C5NR07681A.

[42] GOYAL, Monika; GUPTA, B. R. K. Study of shape, size and temperature-dependent elastic properties of nanomaterials. *Modern Physics Letters B* [online]. 2019, vol. 33, no. 26, pp. 1950310 [visited on 2024-02-11]. ISSN 0217-9849. Available from DOI: 10.1142/S021798491950310X.

[43] SANTHANAM, Venugopal; LIU, Jia; AGARWAL, Rajan; ANDRES, Ronald P. Self-Assembly of Uniform Monolayer Arrays of Nanoparticles. *Langmuir* [online]. 2003, vol. 19, no. 19, pp. 7881–7887 [visited on 2024-02-10]. ISSN 0743-7463. Available from DOI: 10.1021/la0341761.

[44] SALATIN, Sara; MALEKI DIZAJ, Solmaz; YARI KHOSROUSHAHI, Ahmad. Effect of the surface modification, size, and shape on cellular uptake of nanoparticles. *Cell Biology International* [online]. 2015, vol. 39, no. 8, pp. 881–890 [visited on 2024-02-10]. ISSN 1065-6995. Available from DOI: 10.1002/cbin.10459.

[45] LEE, S.-H.; DESHPANDE, R.; PARILLA, P. A.; JONES, K. M.; TO, B.; MAHAN, A. H.; DILLON, A. C. Crystalline WO $_3$ Nanoparticles for Highly Improved Electrochromic Applications. *Advanced Materials* [online]. 2006, vol. 18, no. 6, pp. 763–766 [visited on 2024-02-10]. ISSN 0935-9648. Available from DOI: 10.1002/adma.200501953.

[46] JOG, Rajan; BURGESS, Diane J. Pharmaceutical Amorphous Nanoparticles. *Journal of Pharmaceutical Sciences* [online]. 2017, vol. 106, no. 1, pp. 39–65 [visited on 2024-02-10]. ISSN 00223549. Available from DOI: 10.1016/j.xphs.2016.09.014.

[47] LANGILLE, Mark R.; PERSONICK, Michelle L.; ZHANG, Jian; MIRKIN, Chad A. Defining Rules for the Shape Evolution of Gold Nanoparticles. *Journal of the American Chemical Society* [online]. 2012, vol. 134, no. 35, pp. 14542–14554 [visited on 2024-05-02]. ISSN 0002-7863. Available from DOI: 10.1021/ja305245g.

[48] QI, W. H.; WANG, M. P.; LIU, Q. H. Shape factor of nonspherical nanoparticles. *Journal of Materials Science* [online]. 2005, vol. 40, no. 9-10, pp. 2737–2739 [visited on 2024-05-02]. ISSN 0022-2461. Available from DOI: 10.1007/s10853-005-2119-0.

[49] CUI, Chun-Hua; YU, Shu-Hong. Engineering Interface and Surface of Noble Metal Nanoparticle Nanotubes toward Enhanced Catalytic Activity for Fuel Cell Applications. *Accounts of Chemical Research* [online]. 2013, vol. 46, no. 7, pp. 1427–1437 [visited on 2024-02-11]. ISSN 0001-4842. Available from DOI: 10.1021/ar300254b.

[50] ZHENG, Z. Q.; YAO, J. D.; WANG, B.; YANG, G. W. Light-controlling, flexible and transparent ethanol gas sensor based on ZnO nanoparticles for wearable devices. *Scientific Reports* [online]. 2015, vol. 5, no. 1, pp. 11070 [visited on 2024-02-11]. ISSN 2045-2322. Available from DOI: 10.1038/srep11070.

[51] BUNZ, Uwe H. F.; ROTELLO, Vincent M. Gold Nanoparticle–Fluorophore Complexes: Sensitive and Discerning "Noses" for Biosystems Sensing. *Angewandte Chemie International Edition* [online]. 2010, vol. 49, no. 19, pp. 3268–3279 [visited on 2024-03-26]. ISSN 1433-7851. Available from DOI: 10.1002/anie.200906928.

[52] JANS, Hilde; HUO, Qun. Gold nanoparticle-enabled biological and chemical detection and analysis. *Chem. Soc. Rev.* [online]. 2012, vol. 41, no. 7, pp. 2849–2866 [visited on 2024-03-06]. ISSN 0306-0012. Available from DOI: 10.1039/C1CS15280G.

[53] HUANG, Xiaohua; JAIN, Prashant K.; EL-SAYED, Ivan H.; EL-SAYED, Mostafa A. Plasmonic photothermal therapy (PPTT) using gold nanoparticles. *Lasers in Medical Science* [online]. 2008, vol. 23, no. 3, pp. 217–228 [visited on 2024-03-05]. ISSN 0268-8921. Available from DOI: 10.1007/s10103-007-0470-x.

[54] AMENDOLA, Vincenzo; PILOT, Roberto; FRASCONI, Marco; MARAGÒ, Onofrio M; IATÌ, Maria Antonia. Surface plasmon resonance in gold nanoparticles: a review. *Journal of Physics: Condensed Matter* [online]. 2017, vol. 29, no. 20, pp. 203002 [visited on 2024-03-04]. ISSN 0953-8984. Available from DOI: 10.1088/1361-648X/aa60f3.

[55] KHLEBTSOV, Nikolai G. Extinction and scattering of light by nonspherical plasmonic particles in absorbing media. *Journal of Quantitative Spectroscopy and Radiative Transfer* [online]. 2022, vol. 280, pp. 108069 [visited on 2024-05-10]. ISSN 00224073. Available from DOI: 10.1016/j.jqsrt.2022.108069.

[56] MUSTAFA, Damra E.; YANG, Tianming; XUAN, Zhou; CHEN, Shizhen; TU, Haiyang; ZHANG, Aidong. Surface Plasmon Coupling Effect of Gold Nanoparticles with Different Shape and Size on Conventional Surface Plasmon Resonance Signal. *Plasmonics* [online]. 2010, vol. 5, no. 3, pp. 221–231 [visited on 2024-05-10]. ISSN 1557-1955. Available from DOI: 10.1007/s11468-010-9141-z.

[57] PILIARIK, Marek; VAISOCHEROVÁ, Hana; HOMOLA, Jiří. Surface Plasmon Resonance Biosensing. In: RASOOLY, Avraham; HEROLD, Keith E. (eds.). *Biosensors and Biodetection*. Totowa, NJ: Humana Press, 2009, pp. 65–88. ISBN 978-1-60327-567-5. Available from DOI: 10.1007/978-1-60327-567-5_5.

[58] TVINGSTEDT, Kristofer; PERSSON, Nils-Krister; INGANÄS, Olle; RAHACHOU, Aliaksandr; ZOZOULENKO, Igor V. Surface plasmon increase absorption in polymer photovoltaic cells. *Applied Physics Letters*. 2007, vol. 91, no. 11, pp. 113514. ISSN 0003-6951. Available from DOI: 10.1063/1.2782910.

[59] TWENEY, Ryan D. Discovering Discovery: How Faraday Found the First Metallic Colloid. *Perspectives on Science* [online]. 2006, vol. 14, no. 1, pp. 97–121 [visited on 2024-03-05]. ISSN 1063-6145. Available from DOI: 10.1162/posc.2006.14.1.97.

[60] BRAUN, Jan. Řízení kvantitativního prvkového složení laserem syntetizovaných nanokoloidů zlato-nikl. Available also from: https://dspace.tul.cz/handle/15240/166140.

[61] XIAO, Junyan; QI, Limin. Surfactant-assisted, shape-controlled synthesis of gold nanocrystals. *Nanoscale*. 2011, vol. 3, no. 4, pp. 1383–1396. Available from DOI: 10.1039/C0NR00814A.

[62] ZHANG, Nancy Meng Ying; QI, Miao; WANG, Zhixun; WANG, Zhe; CHEN, Mengxiao; LI, Kaiwei; SHUM, Ping; WEI, Lei. One-step synthesis of cyclodextrin-capped gold nanoparticles for ultra-sensitive and highly-integrated plasmonic biosensors. *Sensors and Actuators B: Chemical* [online]. 2019, vol. 286, pp. 429–436 [visited on 2024-05-10]. ISSN 09254005. Available from DOI: 10.1016/j.snb.2019.01.166.

[63] BAIG, Nadeem; KAMMAKAKAM, Irshad; FALATH, Wail. Nanomaterials: a review of synthesis methods, properties, recent progress, and challenges. *Materials Advances* [online]. 2021, vol. 2, no. 6, pp. 1821–1871 [visited on 2024-03-20]. ISSN 2633-5409. Available from DOI: 10.1039/D0MA00807A.

[64] ZENG, Haibo; DU, Xi-Wen; SINGH, Subhash C.; KULINICH, Sergei A.; YANG, Shikuan; HE, Jianping; CAI, Weiping. Nanomaterials via Laser Ablation/Irradiation in Liquid: A Review. *Advanced Functional Materials* [online]. 2012, vol. 22, no. 7, pp. 1333–1353 [visited on 2023-11-27]. ISSN 1616-301X. Available from DOI: 10.1002/adfm.201102295.

[65] DELL'AGLIO, Marcella; GAUDIUSO, Rosalba; ELRASHEDY, Remah; DE PASCALE, Olga; PALAZZO, Gerardo; DE GIACOMO, Alessandro. Collinear double pulse laser ablation in water for the production of silver nanoparticles. *Phys. Chem. Chem. Phys.* 2013, vol. 15, no. 48, pp. 20868–20875. Available from DOI: 10.1039/C3CP54194K.

[66] COMPAGNINI, G.; SCALISI, A. A.; PUGLISI, O. Production of gold nanoparticles by laser ablation in liquid alkanes. *Journal of Applied Physics*. 2003, vol. 94, no. 12, pp. 7874–7877. ISSN 0021-8979. Available from DOI: 10.1063/1.1628830.

[67] MAFUNÉ, Fumitaka; KOHNO, Jun-ya; TAKEDA, Yoshihiro; KONDOW, Tamotsu. Formation of Stable Platinum Nanoparticles by Laser Ablation in Water. *The Journal of Physical Chemistry B* [online]. 2003, vol. 107, no. 18, pp. 4218–4223 [visited on 2024-05-10]. ISSN 1520-6106. Available from DOI: 10.1021/jp021580k.

[68] SENTEIN, Carole; GUIZARD, Benoit; GIRAUD, Sophie; YÉ, Chang; TÉNÉGAL, François. Dispersion and stability of TiO $_2$ nanoparticles synthesized by laser pyrolysis in aqueous suspensions. *Journal of Physics: Conference Series* [online]. 2009, vol. 170, pp. 012013 [visited on 2024-05-10]. ISSN 1742-6596. Available from DOI: 10.1088/1742-6596/170/1/012013.

[69] ZHANG, Dongshi; GÖKCE, Bilal; BARCIKOWSKI, Stephan. Laser Synthesis and Processing of Colloids: Fundamentals and Applications. *Chemical Reviews* [online]. 2017, vol. 117, no. 5, pp. 3990–4103 [visited on 2023-11-22]. ISSN 0009-2665. Available from DOI: 10.1021/acs.chemrev.6b00468.

[70] ABDALLAH, Bc Sabrin. Manipulation of element distribution in laser-synthesized Pd/FeOx nanoparticles. 2022. Available also from: https://knihovna-opac.tul.cz/records/b719d3f3-5e2d-49b0-b184-71c6dc760cd7.

[71] HAVELKA, Bc Ondřej. Laser-generated synthesis of Pd-Ni nanoalloys usable as catalysts. 2021. Available also from: https://dspace.tul.cz/handle/15240/160485.

[72] LIN, X. Z.; LIU, P.; YU, J. M.; YANG, G. W. Synthesis of CuO Nanocrystals and Sequential Assembly of Nanostructures with Shape-Dependent Optical Absorption upon Laser Ablation in Liquid. *The Journal of Physical Chemistry C* [online]. 2009, vol. 113, no. 40, pp. 17543–17547 [visited on 2024-04-02]. ISSN 1932-7447. Available from DOI: 10.1021/jp907237q.

[73] RAZAGHIANPOUR, Mahdieh; HANTEHZADEH, Mohammad Reza; SARI, Amir Hossein; DARABI, Elham. Electric field assisted-laser ablation of cu nanoparticles in ethanol and investigation of their properties. *Optical and Quantum Electronics* [online]. 2022, vol. 54, no. 1, pp. 23 [visited on 2024-04-02]. ISSN 0306-8919. Available from DOI: 10.1007/s11082-021-03286-z.

[74] HAVELKA, Ondřej; ABDALLAH, Sabrin; BRAUN, Jan; ŁUKOWIEC, Dariusz; PLACHÝ, Tomáš; CVEK, Martin; TORRES-MENDIETA, Rafael. Reactive laser ablation in acetone towards phase-controlled nonequilibrium Iron- and Nickel-Bi2O3 nanoalloys. *Applied Surface Science* [online]. 2023, vol. 641, pp. 158503 [visited on 2023-11-25]. ISSN 01694332. Available from DOI: 10.1016/j.apsusc.2023.158503.

[75] PROCHOWICZ, Daniel; KORNOWICZ, Arkadiusz; LEWIŃSKI, Janusz. Interactions of Native Cyclodextrins with Metal Ions and Inorganic Nanoparticles: Fertile Landscape for Chemistry and Materials Science. *Chemical Reviews* [online]. 2017, vol. 117, no. 22, pp. 13461–13501 [visited on 2023-11-22]. ISSN 0009-2665. Available from DOI: 10.1021/acs.chemrev.7b00231.

[76] SEBASTIAN, Neethu; YU, Wan-Chin; BALRAM, Deepak; AL-MUBADDEL, Fahad S.; TAYYAB NOMAN, Muhammad. Functionalization of CNFs surface with -cyclodextrin and decoration of hematite nanoparticles for detection and degradation of toxic fungicide carbendazim. *Applied Surface Science* [online]. 2022, vol. 586, pp. 152666 [visited on 2024-05-10]. ISSN 01694332. Available from DOI: 10.1016/j.apsusc.2022.152666.

[77] LIU, Zhichang; SCHNEEBELI, Severin T.; STODDART, J. Fraser. Second-Sphere Coordination Revisited. *CHIMIA* [online]. 2014, vol. 68, no. 5, pp. 315 [visited on 2023-11-13]. ISSN 2673-2424. Available from DOI: 10.2533/chimia.2014.315.

[78] VERMA, Govinda; MISHRA, Dr Manish. DEVELOPMENT AND OPTIMIZATION OF UV-VIS SPECTROSCOPY- A REVIEW. *World Journal of Pharmaceutical Research*. Vol. 7, no. 11. Available also from: https://wjpr.s3.ap-south-1.amazonaws.com/article_issue/1527938423.pdf.

[79] AU - QUEVEDO, Ana C. et al. UV-Vis Spectroscopic Characterization of Nanomaterials in Aqueous Media. *JoVE*. 2021, no. 176, pp. e61764. ISSN 1940-087X. Available from DOI: 10.3791/61764.

[80] JAIN, Prashant K.; LEE, Kyeong Seok; EL-SAYED, Ivan H.; EL-SAYED, Mostafa A. Calculated Absorption and Scattering Properties of Gold Nanoparticles of Different Size, Shape, and Composition: Applications in Biological Imaging and Biomedicine. *The Journal of Physical Chemistry B* [online]. 2006,

vol. 110, no. 14, pp. 7238–7248 [visited on 2024-05-10]. ISSN 1520-6106. Available from DOI: 10.1021/jp057170o.

[81] BLAKEY, Idriss; MERICAN, Zul; THURECHT, Kristofer J. A Method for Controlling the Aggregation of Gold Nanoparticles: Tuning of Optical and Spectroscopic Properties. *Langmuir* [online]. 2013, vol. 29, no. 26, pp. 8266–8274 [visited on 2024-05-10]. ISSN 0743-7463. Available from DOI: 10.1021/la401361u.

[82] RAY, Tyler R.; LETTIERE, Bethany; DE RUTTE, Joseph; PENNATHUR, Sumita. Quantitative Characterization of the Colloidal Stability of Metallic Nanoparticles Using UV–vis Absorbance Spectroscopy. *Langmuir* [online]. 2015, vol. 31, no. 12, pp. 3577–3586 [visited on 2024-05-10]. ISSN 0743-7463. Available from DOI: 10.1021/la504511j.

[83] ROCHA, Fellipy S.; GOMES, Anderson J.; LUNARDI, Claure N.; KALIAGUINE, Serge; PATIENCE, Gregory S. Experimental methods in chemical engineering: Ultraviolet visible spectroscopy—UV-Vis. *The Canadian Journal of Chemical Engineering*. 2018, vol. 96, no. 12, pp. 2512–2517. Available from DOI: https://doi.org/10.1002/cjce.23344.

[84] AKHTAR, Kalsoom; KHAN, Shahid Ali; KHAN, Sher Bahadar; ASIRI, Abdullah M. Scanning Electron Microscopy: Principle and Applications in Nanomaterials Characterization. In: SHARMA, Surender Kumar (ed.). *Handbook of Materials Characterization*. Cham: Springer International Publishing, 2018, pp. 113–145. ISBN 978-3-319-92955-2. Available from DOI: 10.1007/978-3-319-92955-2_4.

[85] KUMAR, P. Senthil; PAVITHRA, K. Grace; NAUSHAD, Mu. Chapter 4 - Characterization techniques for nanomaterials. In: THOMAS, Sabu; SAKHO, El Hadji Mamour; KALARIKKAL, Nandakumar; OLUWAFEMI, Samuel Oluwatobi; WU, Jihuai (eds.). *Nanomaterials for Solar Cell Applications*. Elsevier, 2019, pp. 97–124. ISBN 978-0-12-813337-8. Available from DOI: https://doi.org/10.1016/B978-0-12-813337-8.00004-7.

[86] AGARWAL, Nipanshu; NAIR, Maya S.; MAZUMDER, Avik; POLURI, Krishna Mohan. Chapter 3 - Characterization of Nanomaterials Using Nuclear Magnetic Resonance Spectroscopy. In: BHAGYARAJ, Sneha Mohan; OLUWAFEMI, Oluwatobi Samuel; KALARIKKAL, Nandakumar; THOMAS, Sabu (eds.). *Characterization of Nanomaterials*. Woodhead Publishing, 2018, pp. 61–102. Micro and Nano Technologies. ISBN 978-0-08-101973-3. Available from DOI: https://doi.org/10.1016/B978-0-08-101973-3.00003-1.

[87] ANDREW, Edward Raymond; RICHARDS, Rex Edward; PACKER, Kenneth John. Magic angle spinning in solid state n.m.r. spectroscopy. *Philosophical Transactions of the Royal Society of London. Series A, Mathematical and Physical Sciences*. 1981, vol. 299, no. 1452, pp. 505–520. Available from DOI: 10.1098/rsta.1981.0032.

[88] MENÉNDEZ-MANJÓN, Ana; WAGENER, Philipp; BARCIKOWSKI, Stephan. Transfer-Matrix Method for Efficient Ablation by Pulsed Laser Ablation and Nanoparticle Generation in Liquids. *The Journal of Physical Chemistry C* [online]. 2011, vol. 115, no. 12, pp. 5108–5114 [visited on 2024-05-07]. ISSN 1932-7447. Available from DOI: 10.1021/jp109370q.

[89] SHIH, Cheng-Yu et al. Two mechanisms of nanoparticle generation in picosecond laser ablation in liquids: the origin of the bimodal size distribution. *Nanoscale* [online]. 2018, vol. 10, no. 15, pp. 6900–6910 [visited on 2023-11-15]. ISSN 2040-3364. Available from DOI: 10.1039/C7NR08614H.

[90] IKUTA, Naoko et al. Structural Analysis of Crystalline R(+)- -Lipoic Acid- -cyclodextrin Complex Based on Microscopic and Spectroscopic Studies. *International Journal of Molecular Sciences*. 2015, vol. 16, no. 10, pp. 24614–24628. ISSN 1422-0067. Available from DOI: 10.3390/ijms161024614.

[91] NAKAMA, Tsuyoshi; OOYA, Tooru; YUI, Nobuhiko. Temperature- and pH-Controlled Hydrogelation of Poly(ethylene glycol)-Grafted Hyaluronic Acid by Inclusion Complexation with -Cyclodextrin. *Polymer Journal*. 2004, vol. 36, no. 4, pp. 338–344. ISSN 1349-0540. Available from DOI: 10.1295/polymj.36.338.

[92] ACHARYA, Debashish; MOHANTA, Bidhan; DEB, Sanjib; SEN, Asoke Kumar. Theoretical prediction of absorbance spectra considering the particle size distribution using Mie theory and their comparison with the experimental UV–Vis spectra of synthesized nanoparticles. *Spectroscopy Letters* [online]. 2018, vol. 51, no. 3, pp. 139–143 [visited on 2024-05-12]. ISSN 0038-7010. Available from DOI: 10.1080/00387010.2018.1442351.

[93] HENDEL, Thomas; WUITHSCHICK, Maria; KETTEMANN, Frieder; BIRNBAUM, Alexander; RADEMANN, Klaus; POLTE, Jörg. In Situ Determination of Colloidal Gold Concentrations with UV–Vis Spectroscopy: Limitations and Perspectives. *Analytical Chemistry* [online]. 2014, vol. 86, no. 22, pp. 11115–11124 [visited on 2024-05-12]. ISSN 0003-2700. Available from DOI: 10.1021/ac502053s.

[94] JURČEK, Ondřej; PUTTREDDY, Rakesh; TOPIĆ, Filip; JURČEK, Pia; ZARABADI-POOR, Pezhman; SCHRÖDER, Hendrik V.; MAREK, Radek; RISSANEN, Kari. Heads or Tails? Sandwich-Type Metallo Complexes of Hexakis(2,3-di-O-methyl)- -cyclodextrin. *Crystal Growth & Design* [online]. 2020, vol. 20, no. 6, pp. 4193–4199 [visited on 2023-11-23]. ISSN 1528-7483. Available from DOI: 10.1021/acs.cgd.0c00532.

[95] PONCHEL, Anne; MONFLIER, Eric. Application of cyclodextrins as second-sphere coordination ligands for gold recovery. *Nature Communications* [online]. 2023, vol. 14, no. 1, pp. 1283 [visited on 2023-11-13]. ISSN 2041-1723. Available from DOI: 10.1038/s41467-023-36700-z.

[96] TORRES-MENDIETA, Rafael; HAVELKA, Ondřej; URBÁNEK, Michal; CVEK, Martin; WACŁAWEK, Stanisław; PADIL, Vinod Vellora Thekkae; JAŠÍKOVÁ, Darina; KOTEK, Michal; ČERNÍK, Miroslav. Laser-assisted synthesis of Fe-Cu oxide nanocrystals. *Applied Surface Science* [online]. 2019, vol. 469, pp. 1007–1015 [visited on 2023-11-13]. ISSN 01694332. Available from DOI: 10.1016/j.apsusc.2018.11.058.

[97] ETTEL, David et al. Laser-synthesized Ag/TiO nanoparticles to integrate catalytic pollutant degradation and antifouling enhancement in nanofibrous membranes for oil–water separation. *Applied Surface Science* [online]. 2021, vol. 564, pp. 150471 [visited on 2023-11-13]. ISSN 01694332. Available from DOI: 10.1016/j.apsusc.2021.150471.